

1 **TemperatureEquilibrium temperature distribution and**
2 **Hadley circulation in an axisymmetric model.**

3

4 **Nazario Tartaglione**

5

6 {School of Science and Technology, University of Camerino, Camerino, Italy} Formattato: Inglese (Stati Uniti)

7

8

9 Correspondence to: N. Tartaglione (nazario.tartaglione@unicam.it)

10

11 **Abstract**

12

13 The impact of the equilibrium temperature distribution, θ_E , on the Hadley circulation
14 simulated by an axisymmetric model is studied. The temperature θ_E distributions that drive the
15 model are modulated here by two parameters, n and k , the former controlling the horizontal
16 broadness and the latter defining change incontrolling the vertical lapse ratestratification of
17 θ_E . In the present study, the changesvariations of the temperature θ_E distribution mimic
18 changes of the energy input of the atmospheric system leaving as an almost invariant the
19 equator-poles θ_E difference. Both equinoctial and time-dependent Hadley circulations are
20 simulated and results compared. The results give evidence that concentrated temperature θ_E
21 distributions enhance the meridional circulation and jet wind speed intensities even with a
22 lower energy input. The meridional circulation and the subtropical jet stream widths are
23 controlled by the broadness of horizontal temperature θ_E rather than the vertical lapse rate
24 kstratification, which is important only when the temperature distribution is concentrated at

Formattato: Tipo di carattere: Non Corsivo

1 the equator. The jet stream position does not show any dependence with n and k , except when
2 the ~~temperature~~ θ_E distribution is very wide and in such a case the jet is located at the mid-
3 latitude and the model temperature clamps to forcing θ_E . Using $n=2$ and $k=1$ we have the
4 formulation of the potential temperature adopted in classical literature. A comparison with
5 other works is performed and our results show that the model running in different
6 configurations (equinoctial, solstitial and time- dependent) yields results similar to one
7 another.

1 1 Introduction

2 The earth's atmosphere is driven by differential heating of the earth's surface. At the
3 equator, where the heating is larger than that at other latitudes, air rises and diverges poleward
4 in the upper troposphere, descending more or less at 30° latitude (subtropics). This circulation
5 is known as Hadley cell. Because of the earth's rotation, this circulation produces two
6 | subtropical jets at about 30° north and 30° south. A poleward shift (Fu and Lin, 2011) and an
7 | enhanced wind speed of these jets (Strong and Davis, 2007) are associated with a possible
8 | Hadley cell widening and strengthening, which has been observed in the last decades (Fu et
9 | al., 2006; Hu and Fu, 2007; Seidel et al., 2008; Johanson and Fu, 2009; Nguyen et al., 2013).

10 There are a few studies suggesting possible causes of these phenomena. One of the
11 theories postulates global warming as a possible cause of Hadley cell widening (Lu et al.,
12 2009). However, the atmosphere is a complex system containing many subsystems interacting
13 with one another and the global warming might not be the only cause that is suggested to
14 explain the widening. Ozone depletion (Lu et al., 2009; Polvani et al., 2011), SST warming
15 | (Chen et al., 2013; Staten et al., 2011) and aerosol (Allen et al., 2012) have also been invoked
16 | to explain the Hadley cell widening.

17 Climate models vary to some extent in their response and the relationship between global
18 warming and Hadley cell is not straightforward. For instance, Lu et al. (2007) found a smaller
19 widening than the observed one. Gitelman et al. (1997) showed that the meridional
20 temperature gradient decreases with increasing global mean temperature and the same result
21 can be found in recent modeling studies (Schaller et al., 2013).

22 Much of our understanding on the Hadley cell comes from theories using simple models
23 (Schneider 1977, Schneider and Lindzen 1977 and Held and Hou 1980, hereafter HH80) and

1 such a simple model will be adopted here in order to understand how temperature
2 distributions can change the Hadley circulation. How much temperature change impacts the
3 real Hadley circulation is not clear yet, perhaps because of discrepancies between
4 observations, reanalysis ([Wellisser et al., 1999](#)) and climate model outputs, although
5 these differences are becoming less marked because of newer observational datasets or
6 correction of the older ones (Sherwood 2008, Titchner et al., 2008, Santer et al., 2008). Hence,
7 it is critical to understand the possible mechanisms behind the cell expansion starting from a
8 simple model.

9 The objective of this study is to analyze the sensitivity of a model of the symmetric
10 circulation to the radiative-convective equilibrium temperature distribution. Our point of
11 departure is the symmetric model used by Cessi (1998), which is a bidimensional model
12 considering atmosphere as a thin spherical shell. This model will be briefly described in Sect.
13 2. The model describes mainly a tropical atmosphere, hence it does not allow for eddies.
14 Although eddies may play a central role in controlling the strength and width of the Hadley
15 cell (e.g. Kim and Lee, 2001; Walker and Schneider, 2006), a symmetric circulation, driven
16 by latitudinal differential heating, can exist even without eddies and it is a robust feature of
17 the atmospheric system (Dima and Wallace, 2003). The temperature distributions used in this
18 study represent some paradigms of tropical atmospheres. Among the possible causes that can
19 change temperature distributions there are El Niño, global warming and change of solar
20 activity. We will show, in Sect. 3, that the energy input is not as important as the
21 [temperature forcing](#) distribution. Our results are consistent with those obtained both by Hou
22 and Lindzen (1992) (hereafter HL92), and recently by Tandon et al. (2013) who performed
23 experiments similar to those described here. The conclusions will be drawn in Sect. 4.

1 2 The model

2 The model used in this study is a bidimensional model of the axis-symmetric atmospheric
3 circulation described in Cessi (1998). The horizontal ~~variable~~coordinate is defined as $y =$
4 $a \sin \phi$ from which we have

5 $c(y) = \cos \phi = \sqrt{(1 - y^2/a^2)}$ (1)

6 where a is the radius of a planet having a rotation rate Ω , the height of atmosphere is
7 prescribed to be H .

8 The model is similar to the Held and Hou model (HH80), but ~~the difference is that, the~~
9 ~~model~~it prescribes a horizontal diffusion ν_H other than the vertical diffusion ν_v . The
10 prognostic variables are the angular momentum M , defined as $M = \Omega a c^2 + u c$ where u
11 represents the zonal velocity; the zonal vorticity ψ_{zz} with the meridional stream function ψ
12 defined by

13
$$\begin{aligned} \frac{\partial_x \psi}{\partial_y \psi} &\equiv w; \quad \partial_y \psi \equiv w; \\ \frac{\partial_z \psi}{\partial_x \psi} &\equiv -cv; \quad \partial_z \psi \equiv -cv \end{aligned}$$

14 (2)

15 and the potential temperature θ that is forced towards a radiative-convective equilibrium
16 temperature θ_E . Starting from the dimensional equations of the angular momentum, zonal
17 vorticity and potential temperature, we will obtain a set of dimensionless equations. The new
18 equations are non-dimensionalized using a scaling that follows Schneider and Lindzen (1977),
19 but the zonal velocity u is scaled with Ωa . A detailed description can be found in Cessi (1998).

20 The non-dimensional model equations are:

21
$$M_t = \frac{1}{R} \left\{ M_{zz} + \mu [c^4 (c^{-2} M)_y]_y \right\} - J(\psi, M) \quad (3a)$$

1 $\psi_{ztt} = \frac{1}{(R^2 E^2)} y c^{-2} (M^2)_z - \frac{1}{c^{-2}} J(\psi, c^{-2} \psi_{zz}) + \frac{1}{(R E^2 c^{-2})} \theta_y + \frac{1}{(R c^{-2})} [c^{-2} \psi_{zzzz} + \mu \psi_{zzyy}]$ (3b)

2 $\theta_t = \frac{1}{R} \{ \theta_{zz} + \mu [c^2 \theta_y]_y + \alpha [\theta_E(y, z) - \theta] \} - J(\psi, \theta)$ (3c)

3 The term $J(A, B) = A_y B_z - A_z B_y$ is the Jacobian.

4 The thermal Rossby number R ; the Ekman number E , the ratio of the horizontal to the vertical
5 viscosity μ and the parameter α are defined as

6 $R \equiv gH \Delta_H / (\Omega^2 a^2); E \equiv \nu_V / (\Omega H^2); \mu \equiv (H^2 / a^2) \nu_H / \nu_V; \alpha \equiv H^2 / (\tau \nu_V)$ (4)

7 The term α is the ratio of the viscous timescale across the depth of the model atmosphere to
8 the relaxation time τ toward the radiative-convective equilibrium.

9 The boundary conditions for the set of Eq. 3 are:

10 $M_z = \gamma(M - c^2), \psi_{zz} = \gamma \psi_z;$
10 $\psi = \theta_z = 0$ at $z = 0;$
10 $M_z = \psi_{zz} = \psi = \theta_z = 0$ at $z = 1.$

11

_____ (5)

12 Where $\gamma = \frac{C_H}{\nu_V}$ is the ratio of the spin-down time due to the drag to the viscous timescale, the
13 bottom drag relaxes the angular momentum M to the local planetary value $\Omega a c^2$ through a
14 drag coefficient $C.$

15 The model flow started from an isothermal state at rest and is maintained by a Newton
16 heating function where the heating rate is proportional to the difference between the model
17 potential temperature and a specified radiative-convective equilibrium temperature
18 distribution, which follows the HH80 one:

19 $\theta_E = \frac{4}{3} - y^2 + \frac{\Delta V}{\Delta H} \left(z - \frac{1}{2} \right).$ (6)

1 We will assume that Eq. 6 is the radiative-convective equilibrium temperature distribution of
2 the control experiment; we define a general form of the Eq. 6 as

3 $\theta_E = \frac{4}{3} - |y|^n + \frac{\Delta V}{\Delta H} \left(z^k - \frac{1}{2} \right)$ (7)

4 Equation 6 is used extensively in dry axisymmetric models (e.g. HH80, Farrell, 1990, Cessi
5 1998) and it is related to the thermal forcing term of the equation system. A statically stable
6 state as a vertical profile of θ_E is also assumed by Eq. 6. HH80 suggested that the impact of
7 latent heat released by water vapor condensation can be incorporated in dry axisymmetric
8 models by modifying the meridional distribution of θ_E . HL92 followed the HH80 argument
9 and altered the concentration of θ_E under the constraint of equal energy input. The resulting θ_E
10 distributions used by HL92 were peaked distribution on and off the equator resulting in a
11 stronger Hadley circulation with respect the circulation obtained applying Eq. 6. Tandon et al.
12 (2013) used narrow and wide thermal forcing to mimic El Niño or global warming effect on a
13 tropical circulation in a Global Circulation Model. On the opposite side, in fact, we can
14 suppose that if a warmer climate, especially in the tropical regions, happens a very weak
15 gradient of the equilibrium temperature θ_E will be more extent in latitude, expanding
16 consequently the tropical region. This is already occurred in the past, especially in the mid
17 Cretaceous and Eocene when the tropics extended up to 60°. This is the so called equable
18 climate (e.g. Greenwood and Wing, 1995) where the horizontal temperature gradient was
19 weaker than the present one. During those geological ages the temperature was generally
20 higher everywhere, but summing up a constant to the temperature does not change the
21 response of this kind of models. The equator-pole temperature gradient was smaller than the
22 present situation, whereas we prescribe equator-pole θ_E gradient at the surface constant. As
23 we shall show afterwards this is necessary to demonstrate that it is the tropical temperature

1 gradient rather than the equator-pole one the driver of the Hadley circulation. Thus, in order to
 2 study systematically these different conditions we adopt the strategy to build forcing functions
 3 dependent on a parameter that controls the θ_E gradient in the tropical regions. Since, with
 4 different horizontal distributions of θ_E we can figure out that even the vertical distribution
 5 could be affected by some physical mechanisms that make the atmosphere more or less stable
 6 than the stratification described by the z component of Eq. 6. The changes of meridional
 7 extension and vertical stability can be obtained by changing the exponents of y and z in Eq. 6
 8 transforming Eq. 6 in the following equation:

$$9 \quad \theta_E = \frac{4}{3} - |y|^n + \frac{\Delta V}{\Delta H} \left(z^k - \frac{1}{2} \right). \quad (7)$$

10 The values n and k control the horizontal homogenization of the temperature and the lapse
 11 rate respectively. When n=2 and k=1 Eq. (7) becomes the reference equilibrium temperature
 12 given in Eq. 6. In many other works (e.g. Schneider 1977, HH80, Caballero et al. 2008), the
 13 considered atmosphere is essentially dry; however the distribution of temperature of a dry
 14 atmosphere can reflect an action of the water vapor condensation (HL92). Tandon et al. (2013)
 15 used narrow and wide thermal forcing to mimic El Niño or global warming effect on a
 16 tropical circulation in a Global Circulation Model.

17 Starting from Eq. 7 a set of experiments were performed changing n and k in such a
 18 way to have a set of numerical results. In order to isolate the contribution of the temperature
 19 distribution on the solution of Eq. 3, a set of parameters will be used:

$$20 \quad a = 6.4 \times 10^6 \text{ m} \quad \Omega = 2\pi/(8.64 \times 10^4) \text{ s}^{-1}$$

Formattato: western, Giustificato,
 Rientro: Prima riga: 0,85 cm,
 SpazioPrima: 6 pt

$$\Delta_H = 1/3 \quad \Delta_V = 1/8$$

$$g = 9.8 \text{ ms}^{-2} \quad C = 0.005 \text{ ms}^{-1}$$

$$H = 8 \times 10^3 m \quad \tau = 20 \text{ days}$$

1 $v_V = 5 \text{ m}^2 \text{s}^{-1}$ $v_H = 1.86 \text{ m}^2 \text{s}^{-1}$ (8)

2 The values n and k control the horizontal distribution of θ_E and its stratification respectively.

3 Small values of n are associated with concentrated θ_E distributions. Increasing n means
4 increasing broadness of the θ_E distribution. A larger value of k increases the vertical stability,
5 especially at upper levels. Thus it comes quite natural to explore the response of Hadley
6 circulation by changing The parameters in Eq. 8 are the same as those used by Cessi (1998).

7 The meridional and vertical gradients are controlled by the parameters n and k , where which
8 control the distribution of θ_E , in closest ranges of 2 and 1 respectively, they vary from 0.5 to 3
9 with a 0.5 step, in such a way that we have a set of 36 simulations. In fact, when $n=2$ and $k=1$
10 Eq. (7) becomes the reference equilibrium temperature given in Eq. 6 and the experiments
11 performed with $n=2$ and $k=1$ will be considered as the reference experiments.

12 The average temperature θ_E along the latitudes and heights are shown in Fig. 1. Heating
13 functions with n value equal to 0.5 should not be regarded as unreal, but merely as a simple
14 way to represent a specific state of the atmosphere. The same assertion is valid for all other
15 parameters. As n increases the average temperature increases as well, but the meridional
16 gradient decreases. High n values represent situations with a model atmosphere temperature
17 homogenized along the meridional direction (Fig. 1a), in the tropical regions.

18 With the prescribed temperature θ_E as stated inspecified by Eq. 7, the temperature θ_E
19 values at the boundaries and its equator-pole difference temperature remain invariant with
20 respect to n and, for a specific k value. The mean temperatureenergy input is not constant
21 here, which differs from HL92, which analyzed the influence of concentration heating
22 perturbing the forcing function $\theta_E(y, z)$ in such a way that its average θ_E averaged over the

Formattato: Tipo di carattere: Non Corsivo

Formattato: western, Giustificato, Rientro: Prima riga: 0,85 cm, SpazioPrima: 6 pt

Formattato: Inglese (Stati Uniti)

Formattato: western, Giustificato, SpazioPrima: 6 pt

1 domain remained constant. It is easily visible in Fig. 1b. Higher n values, keeping k invariant,
2 have higher ~~mean temperatures averaged θ_E~~ at all levels. The same is true for k , with higher k
3 values, for n constant, ~~the mean temperature for; θ_E at~~ each level is always higher than that
4 with lower k values. The pole-equator ~~temperature θ_E~~ difference at upper and lower vertical
5 boundaries are the same for all the experiments, ~~but having the same k , the meridional~~
6 ~~(vertical) temperature gradient averaged θ_E changes as a function of k , for n (θ) constant.~~
7 Whether global warming makes the ~~earthequilibrium~~ temperature distribution narrower or
8 wider is beyond the aim of the paper. One can expect that global warming broadens the
9 temperature distribution, but at the same time it could have an impact above all on the ~~SST~~
10 ~~sea surface temperature (SST)~~ bringing more water in the upper atmosphere which changes
11 the vertical distribution of the temperature in the ~~intertropical convergence zone~~ ~~inter-tropical~~
12 ~~convergence zone (ITCZ). It is supposed that the oceans force the atmosphere, so we have to~~
13 ~~allow for the possibility that increasing SST can change the forcing distribution. Increasing~~
14 ~~uniformly SST might could a poleward expansion as showed by Chen et al. (2013) with an~~
15 ~~aquaplanet model, but in that case the mechanism was supposed to be related mainly to mid-~~
16 ~~latitude eddies rather than a tropical forcing.~~ Since other causes can change the temperature
17 distribution of a planet such as changes in the solar activity for instance, we will focus on the
18 temperature distribution regardless of its cause.

Formattato: Tipo di carattere: Corsivo, Pedice

Formattato: Tipo di carattere: Non Corsivo

19 ~~— Although inIn this model the atmosphere is dry as in many other studies (e.g.~~
20 ~~Schneider 1977, HH80, Caballero et al. 2008), changing the temperature θ_E distribution~~
21 ~~allows for a change in the static stability. Looking at the mean temperature average θ_E along~~
22 ~~the vertical direction, low values of k are related to low values of static stability, especially in~~
23 ~~higher level of the model atmosphere.~~

Formattato: Inglese (Stati Uniti)

Formattato: western, Giustificato, Rientro: Prima riga: 0,85 cm, SpazioPrima: 6 pt

Formattato: Inglese (Stati Uniti)

1 The Brunt–Väisälä frequency $N^2 = \frac{\theta_z}{\theta_{z,1}}$ when the atmosphere reaches the equilibrium
2 will be

Formattato: Inglese (Stati Uniti)

Formattato: western, Giustificato,
Rientro: Prima riga: 0,85 cm,
SpazioDopo: 9,9 pt

Formattato: Inglese (Stati Uniti)

3
$$N^2 = \frac{(gk\Delta_V/\Delta_H z^{(k-1)})}{[4/3 - y^n + \Delta_V/\Delta_H (z^k - 1/2)]}. \quad (98)$$

4 It is clear from Eq. 98 that the Brunt–Väisälä frequency does not depend on n at the poles and
5 equator. On the contrary, it depends on k ; large values of k imply a more stable atmosphere in
6 the upper levels, especially at poles, making the model atmosphere more similar to the real
7 one, simulating in some respects a sort of tropopause. Moreover, this is equivalent to creating
8 a physical sponge layer in the upper levels of the model that will have some effects on the
9 vertical position of stream function maximum.

Formattato: western, Giustificato,
SpazioPrima: 6 pt

Formattato: Inglese (Stati Uniti)

10 Starting from Eq. 7 a set of experiments were performed changing n and k in such a way
11 to have a set of numerical results. In order to isolate the contribution of the θ_E distribution on
12 the solution of Eq. 3, a set of parameters will be used:

Formattato: western, Giustificato,
Rientro: Prima riga: 0,85 cm,
SpazioPrima: 6 pt

13 $a = 6.4 \times 10^6 \text{ m}$ $\Omega = 2\pi/(8.64 \times 10^4) \text{ s}^{-1}$

$\Delta_H = 1/3$ $\Delta_V = 1/8$

$g = 9.8 \text{ ms}^{-2}$ $C = 0.005 \text{ ms}^{-1}$

$H = 8 \times 10^3 \text{ m}$ $\tau = 20 \text{ days}$

14 $v_V = 5 \text{ m}^2 \text{s}^{-1}$ $v_H = 1.86 \text{ m}^2 \text{s}^{-1} \quad (9)$

15 The parameters in Eq. 9 are the same as those used by Cessi (1998).

1 **3 Numerical Results**

2 This section is divided into three subsections, the first showing the results of the model
3 applying the equinoctial condition, when the sun is assumed to be over the equator. The
4 solution is steady as already shown for instance in Cessi (1998). The second subsection will
5 show the results of the model having a ~~temperature~~ θ_E distribution described by Eq. 7 but
6 moving following a seasonal cycle. The case $n=2$ and $k=1$ is discussed in the third subsection
7 in comparison with previous studies.

8 **3.1 Equinoctial conditions**

9 The axially symmetric circulation is forced by axially symmetric heating as in HH80 and
10 many others and as prescribed by Eq. (7). The model started from an isothermal state and it
11 was run for 300 days, even though it reached its equilibrium approximately after 100 days, in
12 order to be sure that the model does not have instabilities in the long run.

13 The absolute value of the maximum stream function intensity at the equilibrium
14 conditions for the 36 experiments is shown in Fig. 2. When $n=0.5$, with k constant, the
15 circulation is always the strongest. ~~The stream function intensity is inversely proportional to~~
16 n (Fig. 2a). With $n=0.5$ the experiment resembles the one described in HL92 where they
17 concentrated the latitudinal extent of heating and this led to a more intense circulation.
18 However, they imposed the forcing function $\theta_E(x, y)$ in such a way that its average over the
19 domain remained the same as in the control experiment, i.e. without changing the energy
20 input. They found that concentration of the heating through a redistribution of heat within the
21 Hadley cell led to a more intense circulation without altering its meridional extent. Instead,
22 here, it is evident from Fig. 1 that the experiment with $n=0.5$ has an energy input lower than
23 the other cases. Nevertheless, the Hadley circulation is always more intense than the other

Formattato: Tipo di carattere: Corsivo

1 cases and contrary to higher n value experiments, the circulation is confined close to the
2 equator. -Thus the results of HL92 are extended to a more general case with a lower energy
3 input. It is worth ~~noting~~noticing the constraint of an equal pole-equator gradient of mean
4 ~~temperature~~ θ_E is assumed here ~~which is different~~differently from HL92 (Fig. 1a).

5 The dependence on k is not as straightforward as the one on n , instead. The stream
6 function reaches the highest value for $n=0.5$ and $k=3$. With a high n values the Hadley cell
7 stream function intensity is lower and the dependence on k loses its importance. In other
8 words, in our model, the symmetric circulation strength is modulated by k only when the
9 equilibrium temperature distribution is concentrated to the equator. 

Formattato: Inglese (Stati Uniti)

10 Figure 2b shows the maximum zonal wind speed as function of n and k , it is inversely
11 proportional to n , the dependence on k is not as clear as the one on n and when $n=3$ it almost
12 vanishes in accordance with the behavior of the maximum stream function. These results are
13 in agreement with HL92, who found a stronger zonal wind when the temperature forcing was
14 concentrated at the equator.

15 Some studies define the border of a Hadley cell as that by the zero line of the 500 hPa
16 stream function (e.g. Frierson et al., 2007). ~~Since~~Since in this kind of model the zero stream
17 function is at the poles, it is problematic to define an edge of the Hadley cell based on the zero
18 stream function. Moreover, the circulation intensity changes greatly in our experiments, so it
19 is problematic to define ~~a width~~an edge of the Hadley cell based on ~~the~~an absolute value of
20 the circulation itself. ~~Moreover the stream function goes to zero in the model only at the poles.~~
21 Hence, we will define the position of the cell equal to the position of the maximum value of
22 stream function, in this way we will study a possible poleward shift of the cell as a function of
23 the two parameters n and k . The ~~width~~edge of the cell ~~will~~might be defined ~~more or less~~ by

1 values of isolines having 1/4 of that are relative with respect to the maximum value, for
2 example 1/4 of the stream function. It is worth noting thatFor the sake of clarity this definition
3 is an operational one and does not resemblefollow the definition used for example by Dima
4 and WallanceWallace (2003) or Frierson et al. (2007).

5 The latitude of the maximum stream function value shows a general dependence on n
6 and k . It increases with n and decreases with k . However, as shown in Fig. 3a, this dependence
7 is not straightforward or linear, although we have a few exceptions, for instance when
8 $k=n=0.5$. Hence in general when n increases, and the total energy input is larger, the stream

9 function is weaker but poleward. This and the Hadley cell moves poleward. Although this
10 result is in agreement with other model outcomes (Lu et al., 2008; Gastineau et al., 2008; and
11 Tandon et al., 2013), it is in contrast with the recent observations where a slight strengthening
12 and widening of the Hadley Circulationcirculation for the past three decades was observed by
13 Liu et al. (2012) and a poleward expansion was also found by Hu and Fu (2007). However,
14 Liu et al. (2012) showed that if the observations start from 1870, the Hadley cell becomes has
15 become more narrow and stronger.

16 The height of the maximum stream function value is confined for almost all the
17 simulations under 2200 m and the general rule is that when n increases, the height of
18 maximum lowers, however a few experiments, those with $k=0.5$ and $n=0.5, 1$ and 1.5 , have
19 the maximum value between 4300 and 5600 m exhibiting an increase in the height with n (Fig.
20 3b).

21 In general, the location of the maximum zonal wind speed does not show any evident
22 relationship with the parameters n and k . It is always confined between 26° and 29° off the
23 equator; however when $n=3$, there is an abrupt transition to about 48° , independently from the

1 k value. In Table 1, we show the latitude of the maximum wind speed when $k=1$ for different
 2 n values.

3 It is worth calculating the prediction of the cell edge following the HH80 assumptions.
 4 HH80 showed that the Hadley cell has a finite width with the edge ending at a specific
 5 latitude ϕ_H and calculated a scaling for this latitude. Starting with the vertically integrated
 6 hydrostatic equation and a balanced zonal wind, HH80 obtained a formulation for θ in the
 7 limit inviscid:

$$8 \bar{\theta}(\phi) = \bar{\theta}(0) - \bar{\theta}_0 \frac{\omega^2 a^2 \sin^4(\phi)}{2gH \cos^2(\phi)} \quad (10)$$

9 Assuming continuity of the potential temperature $\bar{\theta}(\phi_H) = \bar{\theta}_E(\phi_H)$ and conservation of
 10 vertically averaged potential temperature $\int_0^{\phi_H} \bar{\theta} \cos(\phi) d\phi = \int_0^{\phi_H} \bar{\theta}_E \cos(\phi) d\phi$, they found
 11 ϕ_H as a function of the Rossby number R . The hypothesis of continuity and conservation of
 12 potential temperature is equivalent to solving those two equations by means of a geometric
 13 “equal area” construction.

14 For the general case described by Eq. 7, we calculated a similar relationship between ϕ_H
 15 and the Rossby number, assuming the same hypothesis of HH80 described previously.

$$16 R = \left[\frac{(n+1)}{2n} \right] \frac{\left[(y_H^{\frac{n}{2}}/(1-y) + y_H + 1/3y_H^{\frac{3}{2}} - 1/2 \ln((1+y_H)/(1-y_H))) \right]}{y_H^{\frac{n+1}{2}}} \quad (11)$$

17 The n value goes from 0.5 to 3. Equation 11 should be compared with Eq. 17 of HH80. We
 18 represent the solutions of Eq. 11 in Fig. 4. Evidently for $R=0.121$ (that is the Rossby number
 19 used here), there is no agreement when $n=3$ between analytic solution that predicts a smaller
 20 ϕ_H and the numerical one, which differs from all the other solutions that are quite close to one
 21 another.

1 This behavior could be related to the diffusivity. Figure 5 shows the analytic and
2 numerical vertically averaged potential temperature for $n=k=3$. It is evident that not only $\bar{\theta}$ is
3 not conserved when $n=3$ and there is not redistribution of energy, hence the assumption made
4 by HH80 about the continuity and conservation of potential energy and that leads to Eq. 11
5 never takes place in the numerical model for $n=3$. However, when the vertical diffusion is
6 very small or k has low values $\bar{\theta}$ approaches to $\bar{\theta}_E$ (not shown) but the jet streams have their
7 maxima at the mid latitudes.

8 —— Figure 6 shows the stream function and the zonal wind speed for the experiments
9 $n=k=0.5$ (Fig. 6a) and $n=k=3$ (Fig. 6b). The difference between θ_E and θ , once the model
10 reaches the equilibrium, is quite interesting. Figure 4 shows meridional distributions of θ_E
11 and θ for $n=3$ and $k=0.5, 1$ and 3 . In Fig. 4a, θ_E is under θ , when $k=1$ we find θ_E is over θ in a
12 region around the equator (Fig. 4b), with θ_E crossing θ at about 47° , finding again the equal
13 area condition suggested by HH80 and that explains even the jet location, whereas in Fig. 4c,
14 with $k=3$, we can see how θ_E is over θ . Despite these differences in the distributions of θ_E
15 and θ the model produces with these different k values almost the same solution, in terms of
16 circulation strength and jet location. For other values of n the situation is similar, but with
17 more peaked distributions the differences are not so remarkable.

18 We can understand these findings in the light of Cessi (1998) results obtained by
19 expanding the variables M, θ and ψ in power series of R . The term R^2 in nonlinear expansion
20 part, the meridional advection depends on the differences between θ_E and θ , on the cube of the
21 meridional temperature gradient, and linearly on the imposed stratification deducing that for
22 unstable stratifications, this term would appear as a negative diffusivity term. This seems to
23 be the case, in our simulation when $k=0.5$. The thermal energy obtained in the model is larger

1 than the imposed temperature (Fig.4a). Although the stratification imposed by Eq. 7 is stable,
2 i.e. $\frac{\partial \theta_E}{\partial z} > 0$, the second derivative is negative when $k=0.5$ reducing the stability at upper
3 levels, so it can be thought as a way to simulate the effect of the latent heat released by water
4 vapor condensation. In any case the model acts to bring the vertical temperature gradient in a
5 more stable configuration and a Hadley circulation is in any case reproduced demonstrating
6 the robustness of the model.

7 With n getting larger, the θ_E distribution becomes flatter in the tropical region and θ clamps
8 to θ_E . In general, we expect that a vigorous circulation occurs in a fast rotating planet unless
9 the thermal gradient becomes small in the tropics. In such a case the angular momentum
10 homogenization is equivalent to a weakening of the rotation (Cessi, 1998). If the circulation is
11 proportional to the cube of the meridional temperature gradient, it is quite evident that when
12 such a gradient has high values the circulation is vigorously driven by this term, whereas
13 when it approaches to zero it is the term $\theta_E - \theta$ dominates.). The parameter n controls the
14 Hadley cell and jet stream widths. The experiment with $n=k=0.5$ has Hadley cells and jet
15 streams quite narrow. As far as the vertical position of the maximum value of the stream
16 function is concerned, the experiments with $k=0.5, 1$ and 1.5 exhibit particular behavior with
17 respect to the other experiments. The stream function has its maximum at upper levels. It is
18 likely that such a combination of the parameters favors air to move to higher levels with
19 respect to experiments with higher k values.

20 HH80 found that the edge of the Hadley cell was at the mid-latitudes when the planetary
21 rotation was lower than that of the earth. Since this phenomenon is here observed for a wider
22 temperature forcing distribution, this common result may be attributed to a low efficiency in
23 the process of homogenization of momentum and temperature.

Formattato: western, Giustificato,
Rientro: Prima riga: 0,85 cm,
SpazioPrima: 6 pt

1 In order to explain equitable climates like those supposed to be occurred in Cretaceous
2 and Eocene, Farrell (1990) formulated an axisymmetric model starting from the Held and Hou
3 model and a forcing with $n=2$ and $k=1$ where the temperature gradients became flat because
4 of a dissipation term. For high values of n the θ distributions are similar to those obtained by
5 our forcing conditions. In some respects, flattening of forcing distributions is equivalent to
6 have the same dissipation term in the Farrell (1990) model.

7 Figure 5 shows the stream function and the zonal wind speed for the experiments
8 $n=k=0.5$ (Fig. 5a) and $n=k=3$ (Fig. 5b). The parameter n controls the Hadley cell and jet
9 stream widths. The results show that such with $n=k=0.5$ the Hadley cell and jet streams are
10 quite narrow. As far as the vertical position of the maximum value of the stream function is
11 concerned, the experiments with $k=0.5, 1$ and 1.5 exhibit particular behavior with respect to
12 the other experiments. The stream function has its maximum at upper levels. This is related to
13 the different stratification imposed by the parameter k . Stratification with low values of k
14 favor air to move to higher levels with respect to experiments with higher k values.

16 3.2 Time-dependent simulations

17 Since heating depends on solar irradiation, it is of interest to analyze the solutions
18 obtained by the annually periodic thermal forcing and to compare it with the steady solutions
19 described previously in this paper. Starting from Eq. (7), we can formulate ~~an equilibrium~~
20 temperature distribution having the maximum heating off the equator at latitude $-y_0$:

$$21 \quad \theta_E = \frac{4}{3} - |y - y_0|^n + \frac{4v}{4H} \left(z^k - \frac{1}{2} \right).$$

22 (4210)

1 where y_0 in Eq. (9) is dependent on time according to

2
$$y_0(t) = \sin\left(\frac{\varphi_0\pi}{180}\right) \cdot \sin\left(\frac{2\pi t}{360\text{days}}\right)$$

3 (4311)

4 where φ_0 is the maximum latitude off the equator where heating is maximum. Equations 4211
5 and 4312 are the same used by Fang and Tung (1999) with the choice of maximum extension
6 of φ_0 consistent with the choice of Lindzen and Hou (1988), i.e. $\varphi_0 = 6^\circ$. A prescribed
7 equilibrium temperature varying seasonally makes the simulations more realistic. As
8 described previously, here we will focus on the average and maximum values, in absolute
9 terms, of the stream function and zonal speed obtained during 360 days of simulations. The
10 averaged values are obtained in these cases by averaging the outputs obtained every 30 days,
11 starting from the minimum corresponding to the summer Hadley cell in the boreal hemisphere.

12 The annual averages of the time-dependent and equinoctial circulations shows that
13 maximum stream ~~function-functions~~ and zonal wind speeds behave quite similarly ~~in the~~
14 ~~annual averages of the time-dependent and equinoctial circulations. Nevertheless the time-~~
15 ~~dependent solutions never attain the symmetric circulation obtained by averaging the single~~
16 ~~snapshots (Fig. 7). Even the real earth circulation never reaches the mean6), nevertheless the~~
17 ~~instantaneous~~ Hadley circulation, ~~even because of eddies, but symmetric Hadley cells are~~
18 ~~visible in almost never resembles~~ the ~~averagemodeled~~ circulation (Fang and Tung, 1999) as
19 ~~well as the real one~~ (Dima and Wallace, 2003).

20 The maximum stream function is obtained here ~~by the when~~ $k=n=0.5$ (Fig. 7a6a). In
21 general, for $k=0.5$, we have stronger circulations and winds. It has confirmed the tendency to
22 a weaker stream function and wind speed when n increases. However, the circulation strength
23 expressed as averaged value is weaker ~~in than~~ the time-dependent solution, when n is low and

1 k is high, otherwise it is stronger, but it is never twice as strong as that of the equinoctial
2 solution as found by Fang and Tung (1999). When $n=2$ and $k=1$ it ~~appears more is~~ consistent
3 with the results of Walker and Schneider (2005) as discussed in the Subsect. 3.3. The
4 maximum zonal wind speed shows a behavior slightly different from the stream function
5 intensity; there is a clear dependence on n and k . For example, there is not an analog
6 maximum when $n=0.5$ and $k=3$ found in the steady solution and thus for other k values where
7 the stream function has a relative maximum. With high k value the static stability is high ~~at~~
8 upper levels and the maximum of circulation ~~remains~~ confined to lower levels prevents air
9 upwelling at the high levels. Thus, the transfer of momentum to high level is less effective
10 with respect to the case $k=0.5$ where it is favored ~~is~~ instead.

11 The meridional position and the height of the stream function maximum shows that there
12 is no clear dependency on n and k (Fig. 87). The difference between the time-dependent
13 simulations and the average of the ~~non-time-dependent simulations~~ steady solutions is quite
14 interesting. It is to be noticed that the latitude of the stream function maximum in the time-
15 dependent solution is in the range of 12.5° and 16° (Fig. 8a7a), whereas in the equinoctial
16 solutions the correspondent latitude is within a ~~larger~~ range. It is probable that this more
17 narrow interval is due to the averaging operation. The maximum stream function is located at
18 higher levels, between 4500 and 6000 for n less than 2.5. Otherwise the maximum is
19 positioned under 2500 m except when $n=3$ and $k=0.5$ (Fig. 8b7b).

20 More than the steady solution, it is evident that the height of the maximum stream
21 function is lower when $k=3$. In the steady solution this phenomenon is not that evident. When
22 $k=3$, the vertical gradient of ~~the potential temperature~~ θ_E is higher in upper levels and it
23 prevents, evidently more than the equinoctial solution, air from moving higher leaving

1 circulation occurring at lower levels. The case $k=3$ is equivalent to imposing a “natural”
2 sponge layer at the top of the model. Thus it does not come as a surprise that the maximum
3 stream function is lower than those observed in simulations with other k values. This result is
4 analogous to that of Walker and Schneider (2005) that removed the maximum stream function
5 at higher levels found by Lindzen and Hou (1988) adopting a numerical sponge layer at the
6 top of the model. A comparison with previous works of the simulations with $n=2$ and $k=1$ will
7 be discussed in the Subsect. 3.3.

8 The position of the jet stream is almost similar to the one observed in the steady solution.
9 It is confined between 28° and 30° , with latitude of averaged jet remaining almost at the same
10 place—~~or moving equatorward with n~~ , except when $n=3$ the jets are located at about 44°
11 confirming the abrupt transition of the jet stream position when $n=3$ already found for the
12 equinoctial experiment. Fu and Lin (2011) suggest that the jets moved poleward of about 1°
13 per decade in the last several years but Strong and Davis (2007) observed that Northern
14 hemisphere subtropical jet shifted poleward over the east Pacific, while an equatorward shift
15 of the subtropical jet was found over the Atlantic basin. Excluding the case $n=3$, all the other
16 subtropical jets in the different experiments have the position of the maximum very close to
17 one another and the shifting range is very limited. ~~However, when we use the jet latitude to~~
18 ~~define the edge of the Hadley cell, there is no significant shift but when $n=3$. This appears to~~
19 ~~be in contrast with the Held and Hou model. Thus, when a vigorous circulation occurs the jet~~
20 ~~location must be located at about 30° , whereas reducing too much the tropical gradient the~~
21 ~~process of homogenization becomes weaker like in a slow rotating planet and this is~~
22 ~~confirmed in the time-dependent solution.~~ Both Tandon et al. (2013) and Kang and Polvani
23 (2011) found a discrepancy in this area with the jets that do not follow the Hadley cell edge.
24 In an axisymmetric model, defining the Hadley edge as a function of the stream function and

1 | [connecting it to the jet location is problematic because of lacking of a zero value of the stream](#)
2 | [function.](#)

3 | Figure 98 shows the annually averaged circulation for the same cases as shown in Fig. 65,
4 | which is obtained by annually averaged heating. It is impressive how the steady and time-
5 | dependent solutions resemble each other. As in Fang and Tung (1999) the annual mean
6 | meridional circulation has the same extent, but differently from them the strength of the
7 | annual mean circulation of the time-dependent solution is almost the same of the steady
8 | solution.

9 | When the heating center is off the equator the intensity of the winter cell is stronger,
10 | whereas the cell of the summer hemisphere is weak and sometimes almost absent. Figures
11 | [409](#) and [410](#) show the maxima of the stream function and zonal wind speed at the winter
12 | solstitial as a function of n and k . The maximum stream function as a function of n and k has
13 | the same configuration of the steady solution. Here, as expected the intensity of the
14 | meridional circulation (Fig. [40a9a](#)) is twice as strong as that of the steady solution. The zonal
15 | wind has a different configuration instead, the maximum zonal wind [speed](#) is obtained when
16 | $n=1$ (Fig. [410](#)).

17 | We can inspect a couple of simulations when the stream function reaches its maximum
18 | in the boreal hemisphere. Figure [4211](#) shows the stream function and the zonal wind speed
19 | when $n=2$ and $k=0.5$ (Fig. [42a11a, b](#)) and $n=2$ and $k=3$ (Fig. [42b11c, d](#)). When $k=0.5$ (upper
20 | panels) the boreal (winter) circulation is much stronger when $k=0.5$, with the austral (summer)
21 | circulation almost absent. The vertical extent is larger and the maximum is located at higher
22 | levels. The summer and winter jets are both more intense than their counterparts for $k=3$. The
23 | tropical easterly winds are in this case stronger than those for $k=3$ (13.8 ms^{-1} vs 11.4 ms^{-1}) and

1 the easterly region is also wider. When $k=3$, it is noted that the ~~borealwinter~~ cell is located
2 closer to the equator than the ~~australsummer~~ cell (not easily visible in the figure when $k=0.5$).

3 **3.3 A discussion on the case $n=2$ $k=1$**

4 When $n=2$ and $k=1$, corresponding to the classic case discussed in many studies, we
5 found that the time-dependent solution is only slightly stronger than the steady solution.
6 Lindzen and Hou (1988) proposed a study of the Hadley circulation in which the maximum
7 heating was 6° off the equator. In their non-time-dependent model, the solution showed an
8 average circulation much stronger by a factor 15 for $\phi_0 = 6^\circ$ with respect to the equinoctial
9 solution. ~~–~~Lindzen and Hou (1988) suggested that this exceptional strength was due to a
10 nonlinear amplification of the annually averaged response to seasonally varying heating,
11 although Dima and Wallace (2003) in a study on the seasonality of the Hadley circulation did
12 not observe any nonlinear amplification.

13 With the parameters used for equinoctial and time-dependent simulations we performed
14 an experiment like that of Lindzen and Hou (1988), with $\phi_0 = 6^\circ$ that will be referred to as
15 solstitial experiment. We found that the winter circulation is stronger by a factor three with
16 respect to the steady solution obtained with the equinoctial heating consistent with the result
17 of the axisymmetric model in Walker and Schneider (2005). However, the average circulation,
18 obtained by averaging two solstitial experiments, with $-\phi_0 = 6^\circ$ and $-\phi_0 = -6^\circ$, respectively
19 is only 1.5 times stronger than the steady solution with $\phi_0 = 0^\circ$ and it has a maximum in the
20 upper levels of the model domain as in Lindzen and Hou (1988). We suggest that this
21 maximum is due to a numerical effect caused by averaging the single solstitial experiments
22 rather than a spurious effect caused by the rigid lid as suggested in Walker and Schneider
23 (2005), even though a sponge layer actually lowers ~~this~~the maximum stream function height

1 and we can see the effects of a stronger vertical gradient in the upper levels especially in the
2 time-dependent solution (cf Fig. 3 and Fig. 9-7). Single solstitial experiments did not show a
3 maximum in upper levels and so the equinoctial and time-dependent experiments (Fig. 43-12).
4 Consequently the only operation performed to produce Fig. 43-12c, which exhibits the upper
5 levels maxima was to average the two solstitial experiments, which causes the maximum at
6 upper levels.

7 Finally, we notice that comparing a time-dependent solution with $\varphi_0 = 6^\circ$ with the
8 equivalent steady solution having the heating off the equator is not properly correct, since for
9 the time-dependent model φ_0 represents only the maximum extension of heating, hence a
10 more correct comparison between time and no time-dependent solutions should be performed
11 with the time-dependent solution having $\varphi_0 = 3^\circ$. In such a case, the average solution is only
12 slightly weaker than the Hadley circulation driven by annually averaged heating or by a time-
13 dependent heating which does not show any maximum in the upper levels. Thus, the results of
14 equinoctial, time-dependent and solstitial ($\varphi_0 = 3^\circ$) experiments are mutually consistent.

15 4 Conclusions

16 The temperature distribution forcing of an Earth-like planet can change for several
17 reasons. For instance, a change of the temperature forcing distribution can be caused by
18 different factors such as global warming or long-term variation of solar activity.

19 Under the assumption of an equal equator-pole difference at the surface we used an
20 axisymmetric model to study the sensitivity of the tropical atmosphere to different
21 temperature θ_E distributions modulated by two parameters, n that controls the broadness of the
22 distribution and k that modulates how the temperature θ_E is distributed vertically. Equinoctial
23 and time-dependent solutions were simulated and compared. Moreover for the case $n=2$ and

1 $k=1$, corresponding to the classical distribution used in literature, a few solstitial experiments
2 were also run. When $n=2$ and $k=1$, the annually averaged circulation of equinoctial, time-
3 dependent and solstitial experiments are quite close to one another, consistent with the results
4 of Walker and Schneider (20062005). However, the results differ from those of Lindzen and
5 Hou (1988) and Fang and Tung (1999). As in all those works the maximum of the stream
6 function of the solstitial experiment ~~appears to be is~~ at upper levels, but it seems to be related
7 to a spurious effect of the averaging operation rather than a spurious effect due to the rigid lid.

8 The results provide evidence that concentrated equilibrium temperature distributions
9 enhance the meridional circulation and jet wind speed intensities, confirming findings of
10 Lindzen and Hou (1988) even though these authors imposed the same energy input. However,
11 in the present study the concentrated distribution at the equator has lower energy input.

12 The width of the Hadley cell is proportional to n , but when the cell width increases its
13 intensity decreases. ~~The~~Since the equator-pole gradient is the same for all the experiments;
14 ~~hence with the same~~ k ; it ~~is evident that~~ the gradient ~~equator subtropic that in the tropical~~
15 ~~region~~ controls the circulation strength. ~~Even~~ k , ~~hence the lapse rate, The term~~ k controlling the
16 ~~imposed stratification has influence on the actual temperature distribution that can differ~~
17 ~~remarkably from~~ θ_E ~~distribution.~~

18 Vertical stratification is important in determining the position and intensity of the Hadley
19 cell and jet when n is low, whereas k loses its importance when the ~~temperature~~ θ_E distribution
20 is wider. This latter result is consistent with results of Tandon et al. (2013) who found that the
21 Hadley cell expansion and jet shift had relatively little sensitivity to the change ~~in~~ of the lapse
22 rate. Consequently, the subtropical jet stream intensities are controlled by the broadness of
23 horizontal temperature rather than the ~~vertical lapse rate startification~~, with higher values of

Formattato: Rientro: Prima riga: 0,85
cm

1 the jet when the thermal forcing is concentrated to the equator. However, results show that the
2 jet stream position does not show any dependence with n and k , except when the ~~temperature~~
3 θ_E distribution is the widest ($n=3$); in such a case an abrupt change occurs and the maximum
4 of the zonal wind jet is located at mid-latitudes. The analytic study of this model performed
5 by Cessi (1998) suggest that when the meridional gradient becomes too small the process of
6 homogenization of temperature and momentum occurs slowly and the circulation behaves as
7 that of a slow rotating planet.

8

9

10 **Acknowledgements**

11 Helpful discussions with Antonio Speranza, Valerio Lucarini and Renato Vitolo are gratefully
12 acknowledged. The author thanks two anonymous reviewers for their insightful comments on
13 the paper, which helped to improve the manuscript.

Formattato: Tipo di carattere: 16 pt

Formattato: Tipo di carattere: 16 pt,
Grassetto

1 References

2 Allen, R. J., Sherwood, S. C., Norris, J. R., and Zender, C. S.: Recent Northern Hemisphere
3 tropical expansion primarily driven by black carbon and tropospheric ozone. *Nature*, 485,
4 350–354, -2012.

5 Caballero, R., Pierrehumbert, R. T., and Mitchell, J. L.: Axisymmetric, nearly inviscid
6 circulations in non-condensing radiative-convective atmospheres. *Q. J. Roy. Met. Soc.*, 134,
7 1269-1285, 2008.

8 [Cessi, P.: angular momentum and temperature homogenization in the symmetric circulation](#)
9 [of the atmosphere. *J. Atmos. Sci.*, 55, 1997-2015, 1998.](#)

10 [Chen, G., Lu J., and Sun L.: Delineating the eddy–zonal flow interaction in the atmospheric](#)
11 [circulation response to climate forcing: Uniform SST warming in an idealized aquaplanet](#)
12 [Model. *J. Atmos. Sci.*, 70, 2214–2233. doi:<http://dx.doi.org/10.1175/JAS-D-12-0248.1>, 2013.](#)

13 Dima, I. M., and Wallace, J. M.: On the seasonality of the Hadley cell. *J. Atmos. Sci.*, -60, 60,
14 1522-1527, 2003.

15 Fang, M., and Tung, K. K.: Time-dependent nonlinear Hadley circulation. *J. Atmos. Sci.*, 56,
16 1797-1807, 1999.

17 [Farrell, B. F.: 1990: Equable Climate Dynamics. *J. Atmos. Sci.*, 47, 2986–2995. doi:](#)
18 [http://dx.doi.org/10.1175/1520-0469\(1990\)047<2986:ECD>2.0.CO;2](http://dx.doi.org/10.1175/1520-0469(1990)047<2986:ECD>2.0.CO;2), 1990.

19 [Frierson, D. M. W., Lu, J., Chen, G.: Width of the Hadley cell in simple and comprehensive](#)
20 [general circulation models. *Geophys. Res. Lett.*, L18804, 2007.](#)

21 Fu, Q., Johanson, C. M., Wallace, J. M., and Reichler, T.: Enhanced mid-latitude tropospheric

Formattato: Inglese (Stati Uniti)

1 warming in satellite measurements. *Science*, 312, 1179, -2006.

2 Fu, Q., and Lin, P.: Poleward shift of subtropical jets inferred from satellite-observed lower

3 stratospheric temperatures. *J. Climate*, 24, 5597-5603, doi:10.1175/JCLI-D-11-00027.1, 2011.

4 [Gastineau, G., Le Treut, H. Li, L.: Hadley circulation changes under global warming](#)

5 [conditions indicated by coupled climate models Tellus, 60, 863-884. doi:10.1111/j.1600-](#)

6 [0870.2008.00344.x, 2008.](#)

7 Gitelman, A. I., Risbey, J. S., Kass, R. E., and Rosen, R. D.: Trends in the surface meridional

8 temperature gradient. *Geophys. Res. Lett.*, 24, 1243–1246, 1997.

9 [Greenwood, D. R. and Wing, S. L.: Eocene continental climates and latitudinal temperature](#)

10 [gradients, Geology, 23, 1044–1048, 1995.](#)

11 Held, I. M., and Hou, A. Y.: Nonlinear axially symmetric circulation in a nearly inviscid

12 atmosphere. *J. Atmos. Sci.*, 37, 515-533, 1980.

13 Hou, A.Y., and Lindzen, R. S.: The influence of concentrated heating on the Hadley

14 circulation. *J. Atmos. Sci.*, 49, 1233-1241, 1992.

15 Hu, Y., and Fu, Q.: Observed poleward expansion of the Hadley circulation since 1979.

16 *Atmos. Chem. Phys.*, 7, 5229–5236, 2007.

17 Johanson, C. M., and Fu, Q.: Hadley cell widening: Model simulations versus observations. *J.*

18 *Climate*, 22, 2713– 2725, 2009.

19 [Kang, S. M., and Polvani, L. M.: The interannual relationship between the latitude of the](#)

20 [eddy-driven jet and the edge of the Hadley Cell. J. Climate 24 \(2\): 563–68.](#)

21 [doi:10.1175/2010JCLI4077.1, 2011.](#)

1 Kim, H.-K., and Lee, S.: Hadley cell dynamics in a primitive equation model. Part II:
2 Nonaxisymmetric flow. *J. Atmos. Sci.*, 58, 2859–2871, 2001.

3 [Lindzen, R. S., and Hou, A. Y.: Hadley circulations for zonally averaged heating centered off](#)
4 [the Equator, *J. Atmos. Sci.*, 2416-2427, 1988.](#)

5 Liu, J., Song, M., Hu, Y., and Ren, X.: Changes in the strength and width of the Hadley
6 Circulation since 1871. *Clim. Past*, 8, 1169–1175, doi:10.5194/cp-8-1169-2012, 2012.

7 Lu, J., [Chen, G., and Frierson D. M. W.: Response of the zonal mean atmospheric circulation](#)
8 [to El Niño versus global warming. *J. Climate*, 21, 5835–5851.doi:](#)
9 [Circulationcirculation](http://dx.doi.org/10.1175/2008JCLI2200.1, 2008.</p><p>10 Lu, J., Deser, C., and Reichler, T.: Cause of the widening of the tropical belt since 1958.
11 <i>Geophys. Res. Lett.</i>, 36, L03803, doi:10.1029/2008GL036076, 2009.</p><p>12 Lu, J., Vecchi, G. A., and Reichler T.: Expansion of the Hadley cell under global warming.
13 <i>Geophys. Res. Lett.</i> 34, L06805, 2007.</p><p>14 Nguyen, H., Evans, A., Lucas, C., Smith, I., and Timbal, B.: The Hadley
15 <a href=) in [Reanalysesreanalyses](#): Climatology, [Variabilityvariability](#), and
16 [Changechange](#). *J. Climate*, 26, 3357-3376, 2013.

17 Polvani, L. M., Waugh, D. W., Correa, G. J. P., and Son, S.-W.: Stratospheric ozone depletion:
18 the main driver of 20th Century atmospheric circulation changes in the Southern Hemisphere.
19 *J. Climate*, 24, 795-812, doi:10.1175/2010JCLI3772.1, 2011.

20 Santer, B. D., Thorne, P. W., Haimberger, L., Taylor, K. E., Wigley, T. M. L., Lanzante, J. R.,
21 Solomon, S., Free, M., Gleckler, P. J., Jones, P. D., Karl, T. R., Klein, S. A., Mears, C.,

1 Nychka, D., Schmidt, G. A., Sherwood, S. C., and Wentz, F. J.: Consistency of modelled and
2 observed temperature trends in the tropical troposphere. *Int. J. Climatol.*, 28(13), 1703-1722,
3 2008.

4 Schaller, N., Cermak, J., Wild, M., and Knutti, R.: The sensitivity of the modeled energy
5 budget and hydrological cycle to CO₂ and solar forcing. *Earth Syst. Dynam.*, 4, 253-266,
6 doi:10.5194/esd-4-253-2013, 2013.

Formatto: Inglese (Stati Uniti)

7 Schneider E. K.: Axially symmetric steady-state models of the basic state for instability and
8 climate studies. Part II. Nonlinear calculations. *J. Atmos. Sci.*, 34, 280-296, 1977.

9 Schneider, E. K., and Lindzen, R. S.: Axially symmetric steady state models of the basic state
10 of instability and climate studies. Part I: Linearized calculations. *J. Atmos. Sci.*, 34, 253-279,
11 1977.

12 Seidel, D. J., Fu, Q., Randel, W. J., and Reichler, T. J.: Widening of the tropical belt in a
13 changing climate. *Nat. Geosci.*, 1, 21–24, 2008.

14 Sherwood, S. C., Meyer, C. L., Allen, R. J., and Titchner, H. A.: Robust tropospheric
15 warming revealed by iteratively homogenized radiosonde data. *Journal of Climate*, 21(20),
16 5336-5352, 2008.

Formatto: Inglese (Stati Uniti)

17 Staten, P. W., Rutz, J., Reichler, T. and Lu, J.: Breaking down the tropospheric circulation
18 response by forcing. *Clim. Dynam.*, 39, 2361-2375, doi:10.1007/s00382-011-1267-y, 2011.

19 Strong, C., and Davis, R. E.: Winter jet stream trends over the Northern Hemisphere. *Q. J. R.*
20 *Meteorol. Soc.* 133, 2109–2115, 2007.

21 Tandon, N. F., Gerber, E. P., Sobel, A. H. and Polvani, L. M.: Understanding Hadley Cell

1 [expansion versus contraction: Insights from simplified models and implications for recent](#)
2 [observations. Journal of Climate 26 \(12\): 4304–21. doi:10.1175/JCLI-D-12-00598.1, 2013.](#)

3 Titchner, H. A., Thorne, P.W., McCarthy, M.P., Tett, S. F. B., Haimberger L., and Parker, D.
4 E.: Critically reassessing tropospheric temperature trends from radiosondes using realistic
5 validation experiments. *Journal of Climate*, 22(3), 465-485, 2008.

6 Walker, C. C., and Schneider, T.: Response of idealized Hadley circulations to seasonally
7 varying heating. *Geophys. Res. Lett.*, 32, L06813, doi:10.1029/2004GL022304, 2005.

8 Walker, C. C., and Schneider, T.: Eddy influences on Hadley circulations: Simulations with
9 an idealized GCM. *J. Atmos. Sci.*, 63, 3333–3350, 2006.

10 [Waliser, D. E., Shi, Z., Lanzante, J. R., and Oort, A. H.: The Hadley circulation:](#)
11 [assessing NCEP/NCAR reanalysis and sparse in situ estimates. Clim. Dyn., 15, 719-735, 1999.](#)

12
13 —

1 Table 1. Latitudes (in degrees) of the maximum wind speed for the equinoctial and time-
2 dependent solutions when $k=1$ as a function of the parameter n .

3

n	0.5	1	1.5	2	2.5	3
Equinoctial	27.4	28.7	27.4	26.1	28.7	47.7
Time dependent	28.7	28.7	28.7	27.4	27.4	44.4

4

5

1 Figure Captions

2 Figure 1. Meridional (a) and vertical (b) ~~mean average of~~ non-dimensional equilibrium
3 temperature as a function of n with $k=1$ (panels a) and $b>k$ with $n=0.5, 1$ and $k=1.5$ (panel b).

4 Figure 2. Maximum non-dimensional stream function (a) and zonal wind speed [ms^{-1}] (b) as
5 function of parameters n and k for the steady solution.

Formattato: Tipo di carattere: Corsivo

6 Figure 3. Latitude [degree] (a) and Height [m] (b) of maximum non-dimensional stream
7 function.

Formattato: Tipo di carattere: Corsivo

8 Figure 4. ~~Relationship between Rossby number and poleward boundary of the Hadley cell as~~
9 ~~given by Eq. 10, $y_H = \sin \phi_H$. Vertically averaged the θ (blue line) and θ_E (red line) for the~~
10 ~~simulations with $n=3$ and $k=0.5$ (a), $k=1$ (b) and $k=3$ (c),~~

Formattato: Tedesco (Germania)

11 Figure 5. ~~Vertically averaged potential temperature for the simulation with $n=k=3$.~~

12 ~~Figure 6.~~ Non-dimensional stream function (a and econtours) and zonal wind speed (b and
13 d [ms^{-1}] (colors) for the steady cases $n=0.5, k=0.5$ (upper panels a) and $n=3, k=3$ (lower
14 panels b).

Formattato: Tipo di carattere: Corsivo

15 Figure ~~76~~. Maximum of annually averaged non dimensional stream function (a) and zonal
16 wind speed [ms^{-1}] (b) as function of parameters n and k for the time-dependent simulations.

Formattato: Tipo di carattere: Corsivo

17 Figure ~~87~~. Latitude [degree] (a) and Height [m] (b) of maximum annually averaged non-
18 dimensional stream function for the time-dependent solution.

19 Figure ~~98~~. Annually averaged non-dimensional stream function (a and econtours) and zonal
20 wind speed (b and d [ms^{-1}] (colors) for the steady cases $n=0.5, k=0.5$ (upper panels a) and $n=3,$
21 $k=3$ (lower panels b)).

22 ~~Figure 9, Figure 10.~~ Maximum of non-dimensional stream function (a) and zonal wind speed
23 [ms^{-1}] (b) -as function of parameters n and k for the time-dependent simulations.

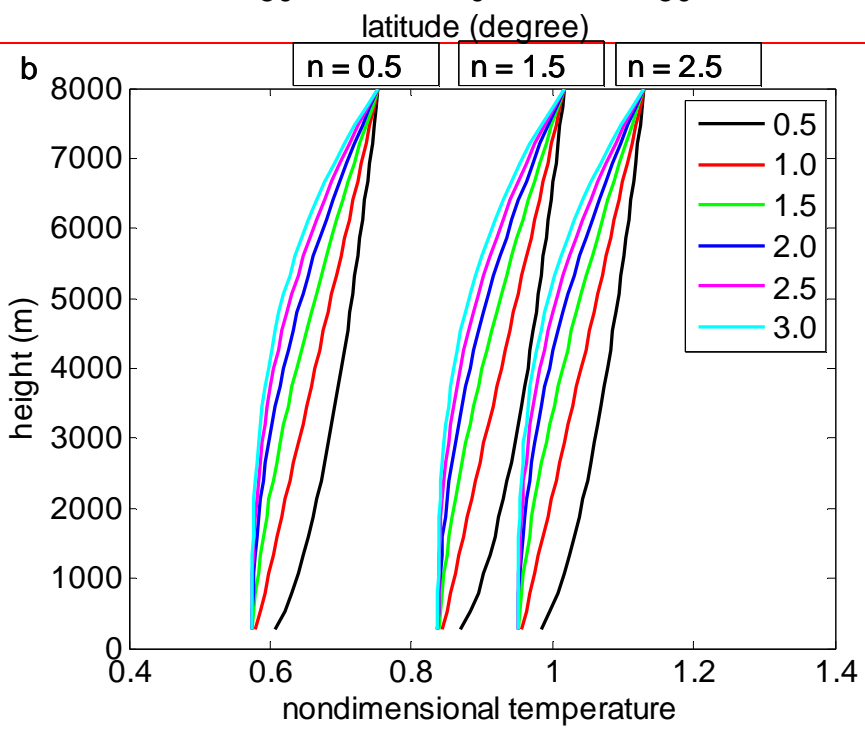
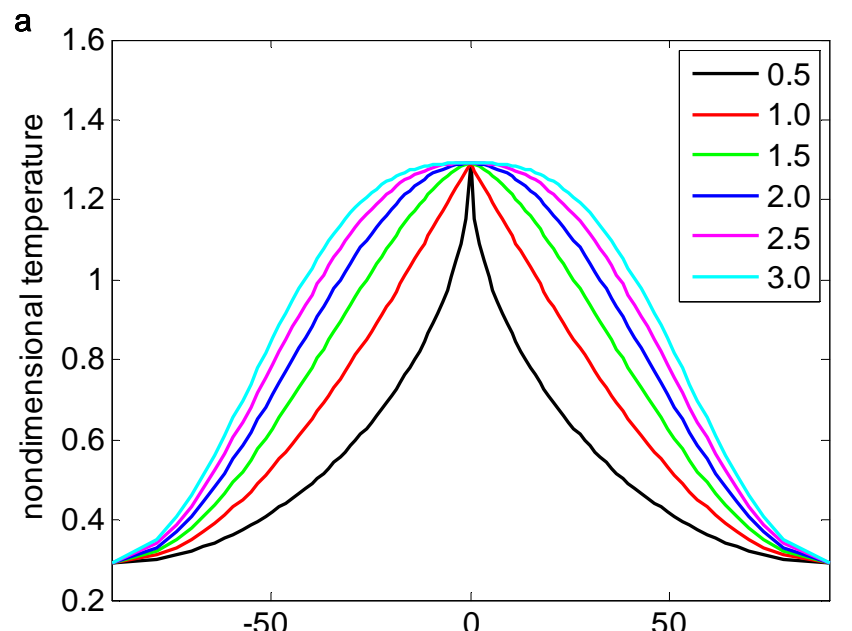
24 ~~Figure 11, Figure 10.~~ Latitude [degree] (a) and Height [m] (b) of maximum non-dimensional
25 stream function for the time-dependent solution.

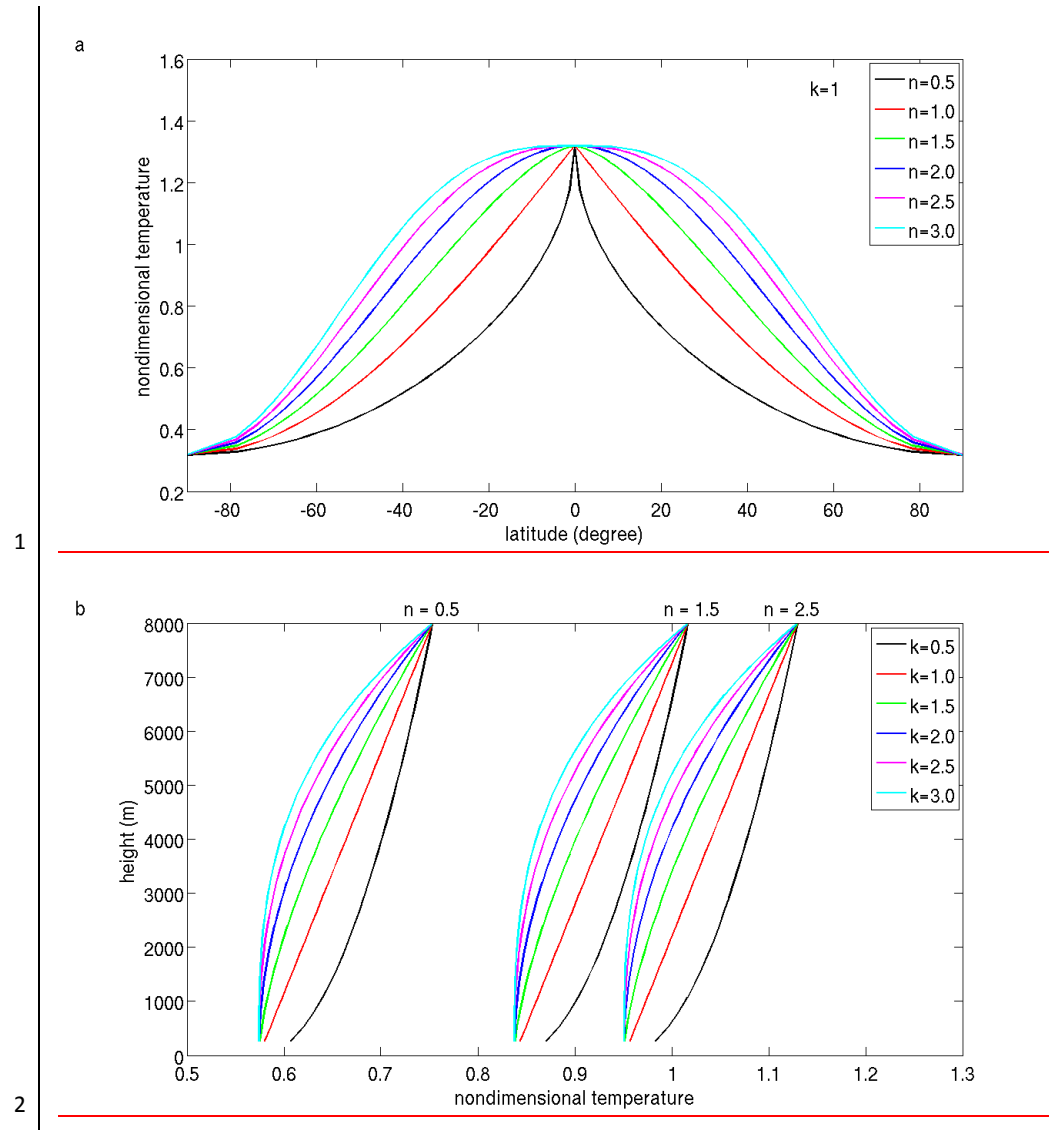
26 Figure ~~42, Winter 11.~~ Boreal winter circulation, non-dimensional stream function (a and c)
27 and zonal wind speed [ms^{-1}] (b and d) ~~when for the time-dependent simulation with~~ $n=2, k=0.5$

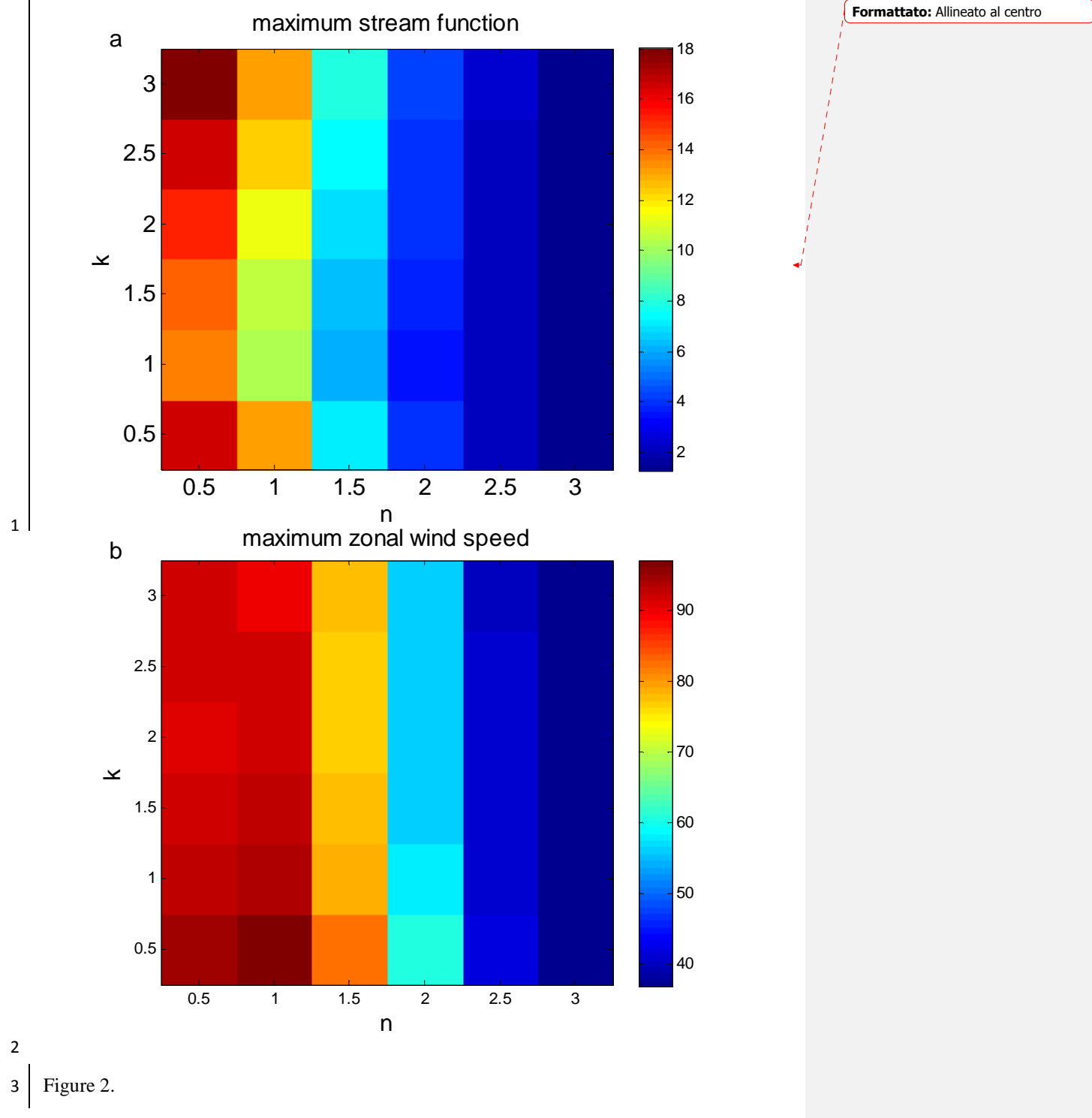
1 (upper panels) and $n=2$, $k=3$ (lower panels) ~~for the time dependent simulation~~. Dashed lines
2 indicate negative values.

3 Figure 1312. Non-dimensional annually averaged stream function (a,e,econtours) and zonal
4 wind speed (b,d,f[ms⁻¹] colors) when $n=2$ and $k=1$ for the steady (a), time-dependent (b) and
5 with the maximum heating 6° off the equator (c). ▲-----

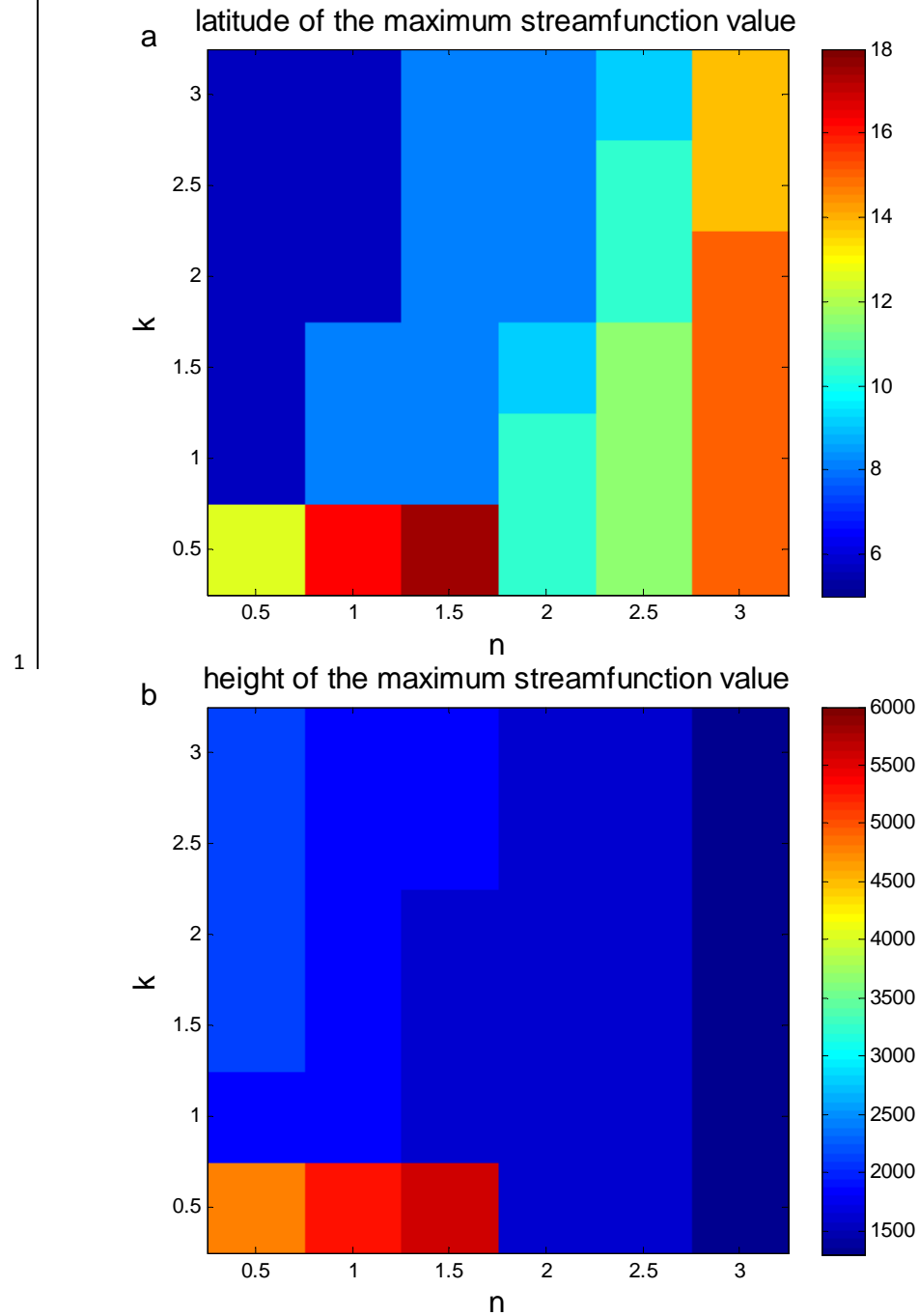
Formattato: Tedesco (Germania)





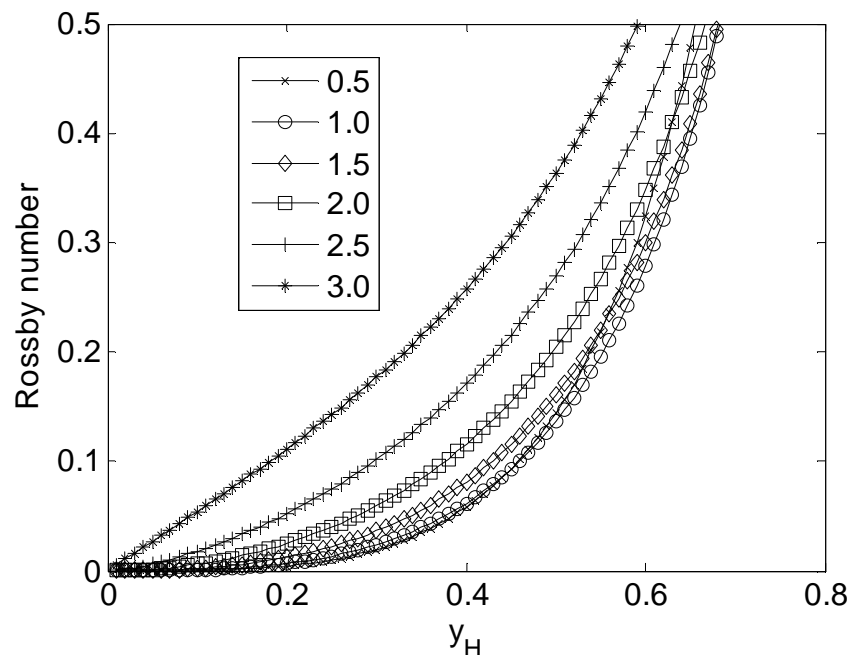


Formattato: Allineato al centro

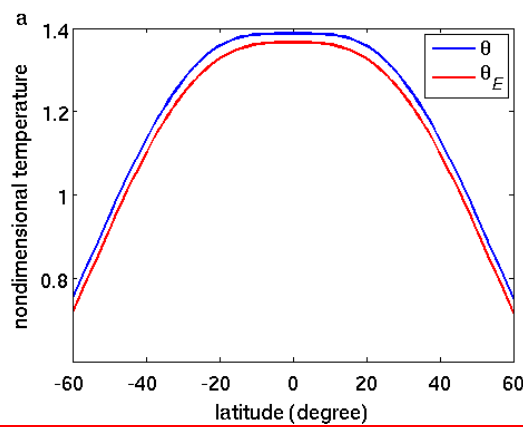


2

3 Figure 3.



1



2

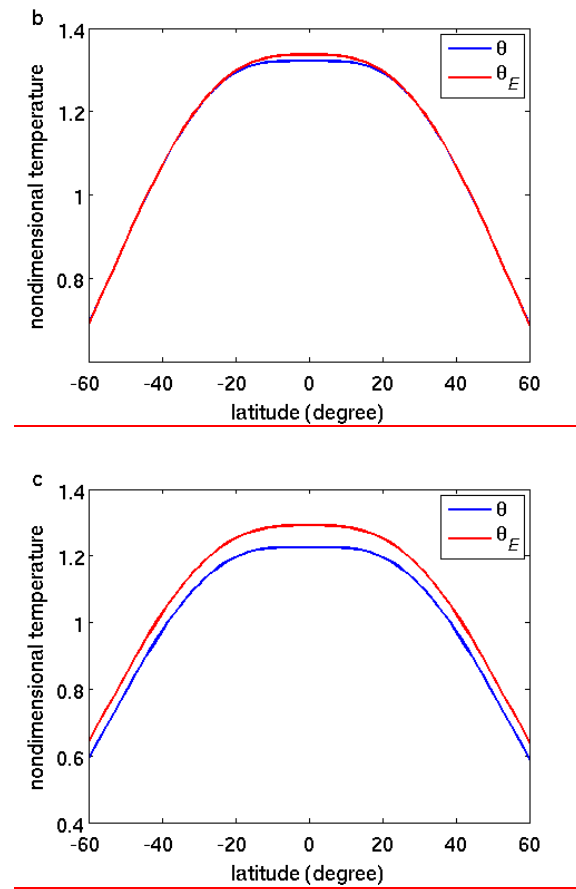
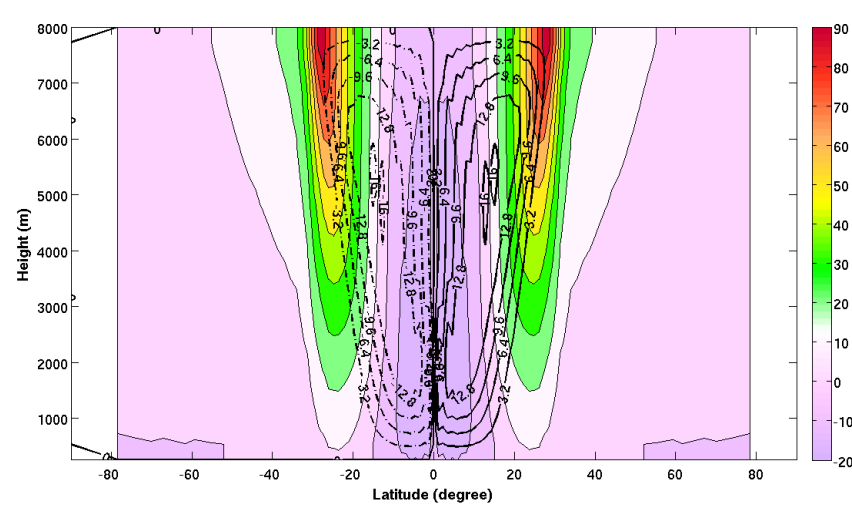
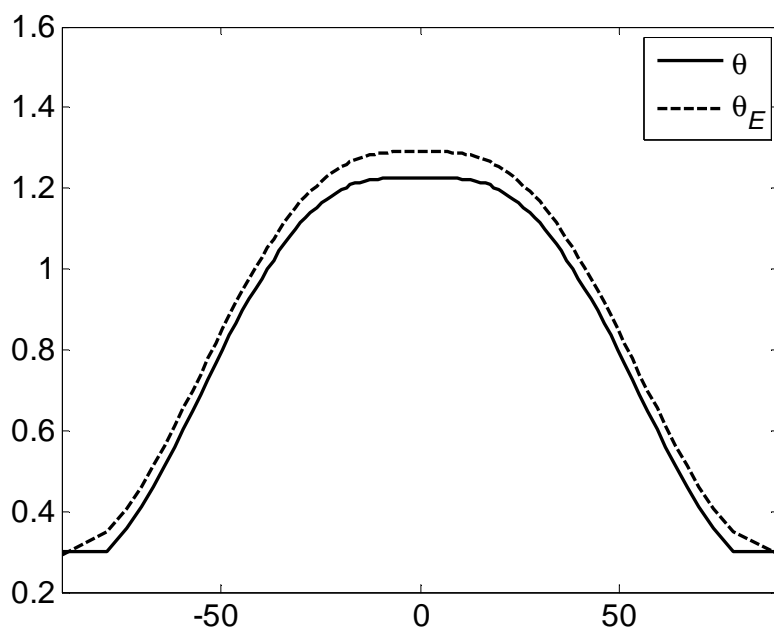
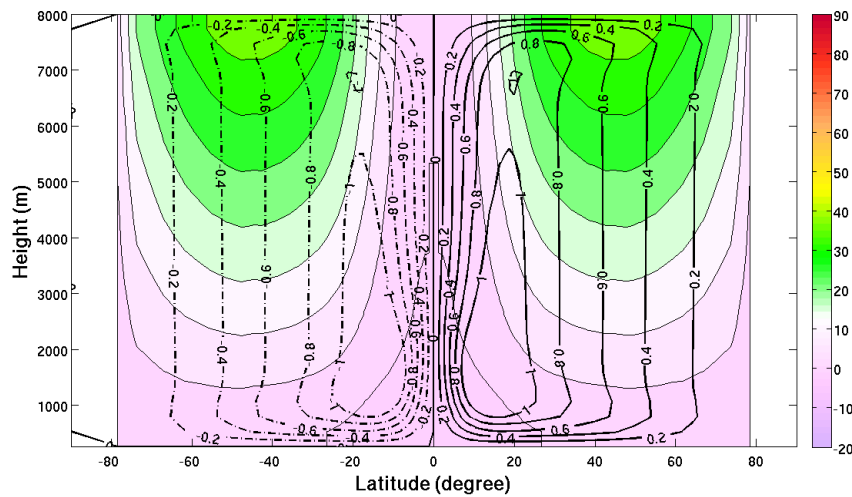


Figure 4.



b

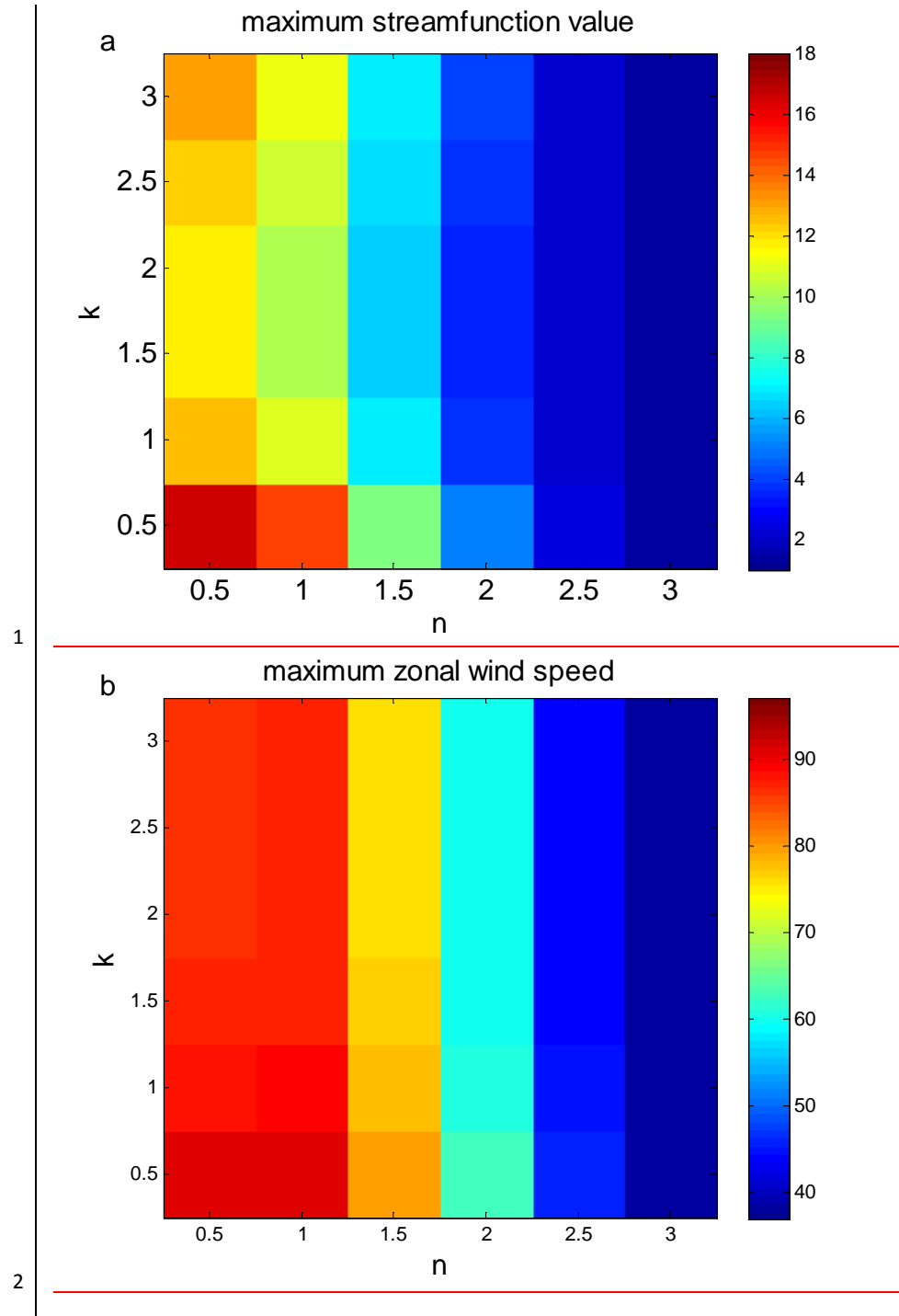


Formattato: Normale

1

2 Figure 5.

Formattato: Tipo di carattere: Times New Roman, 12 pt, Inglese (Stati Uniti)



Formattato: Inglese (Stati Uniti)

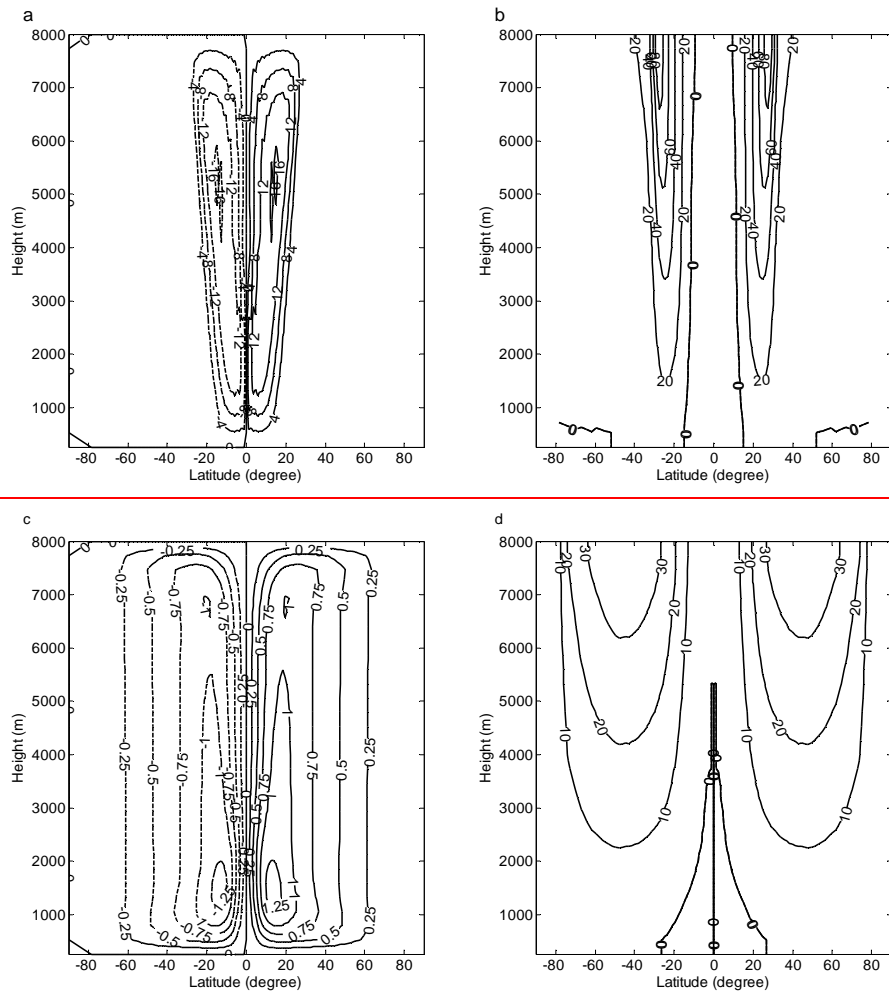
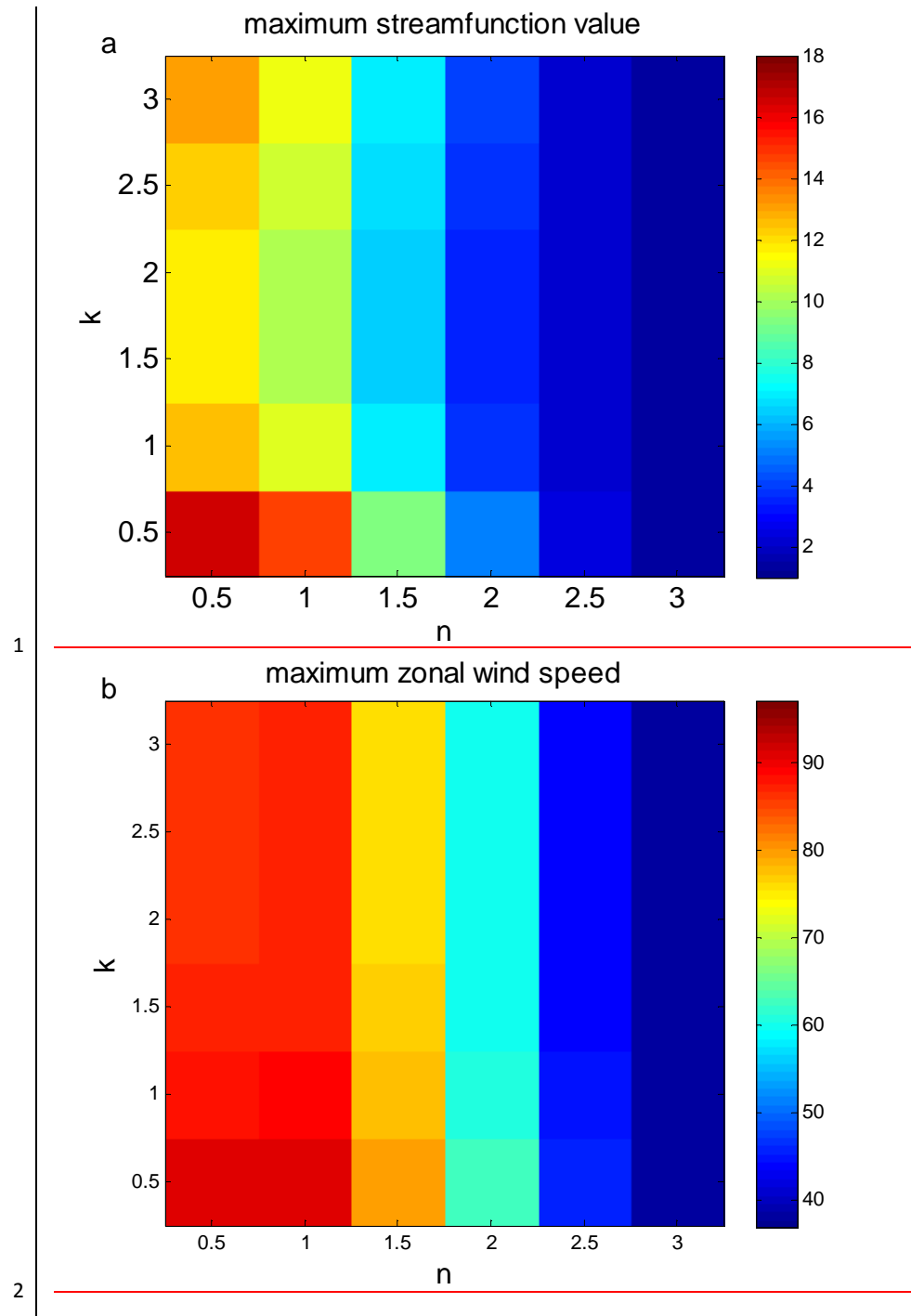
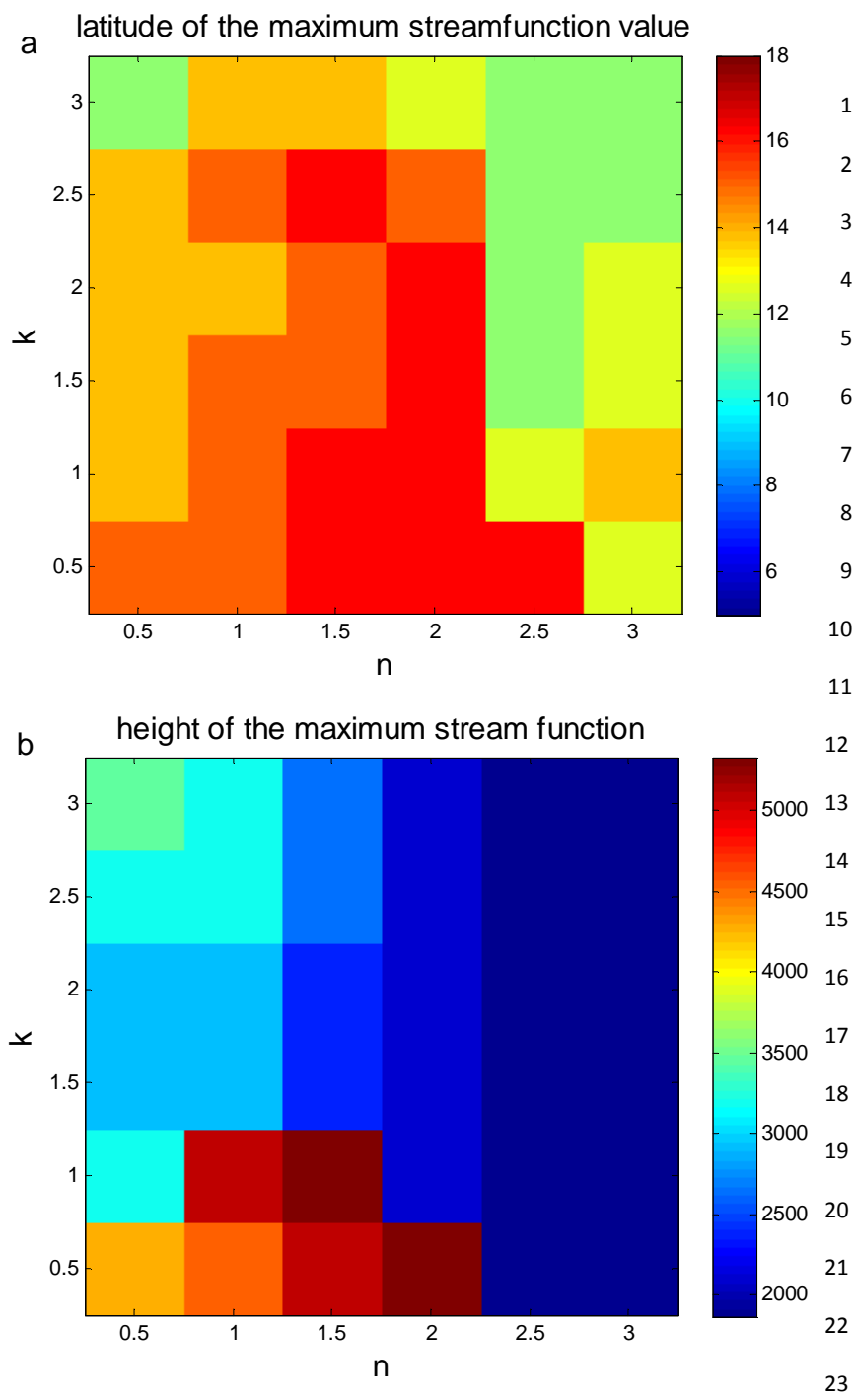
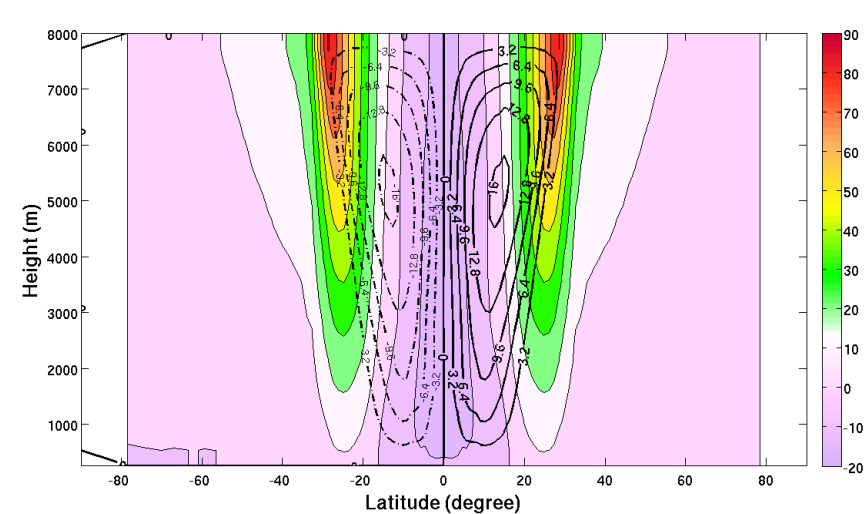


Figure 6.

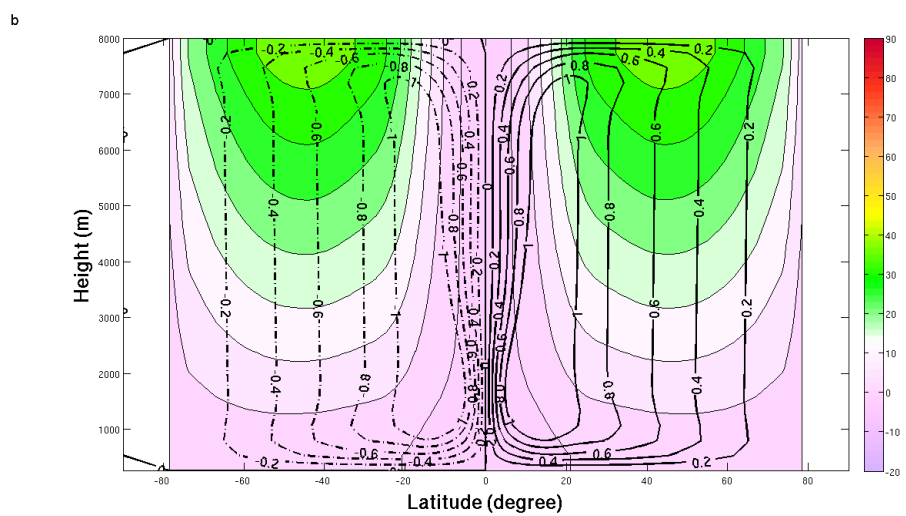




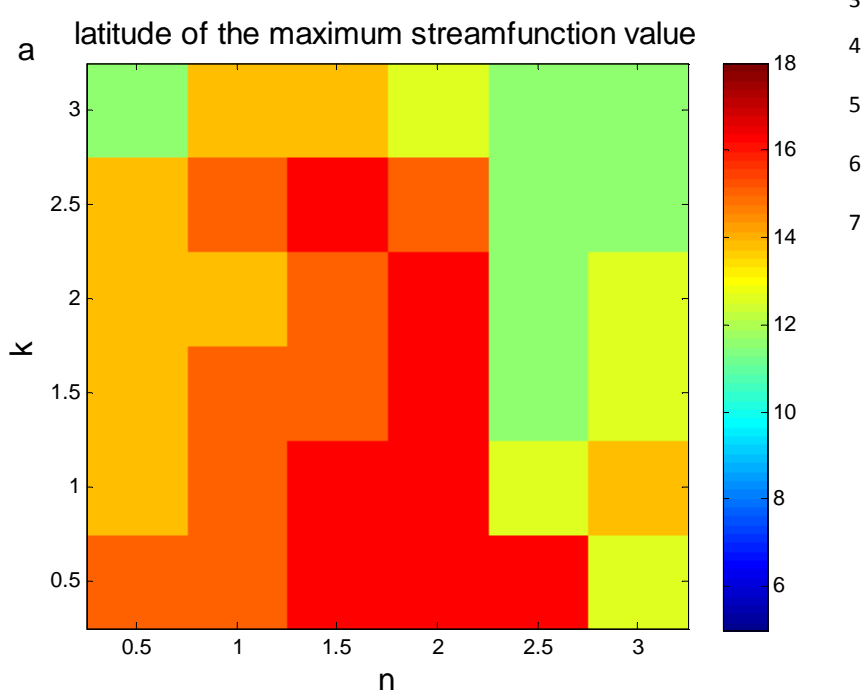
24 Figure 7.



1



2

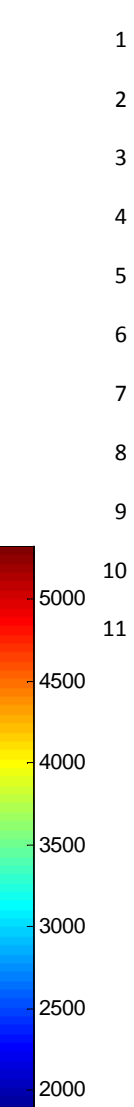


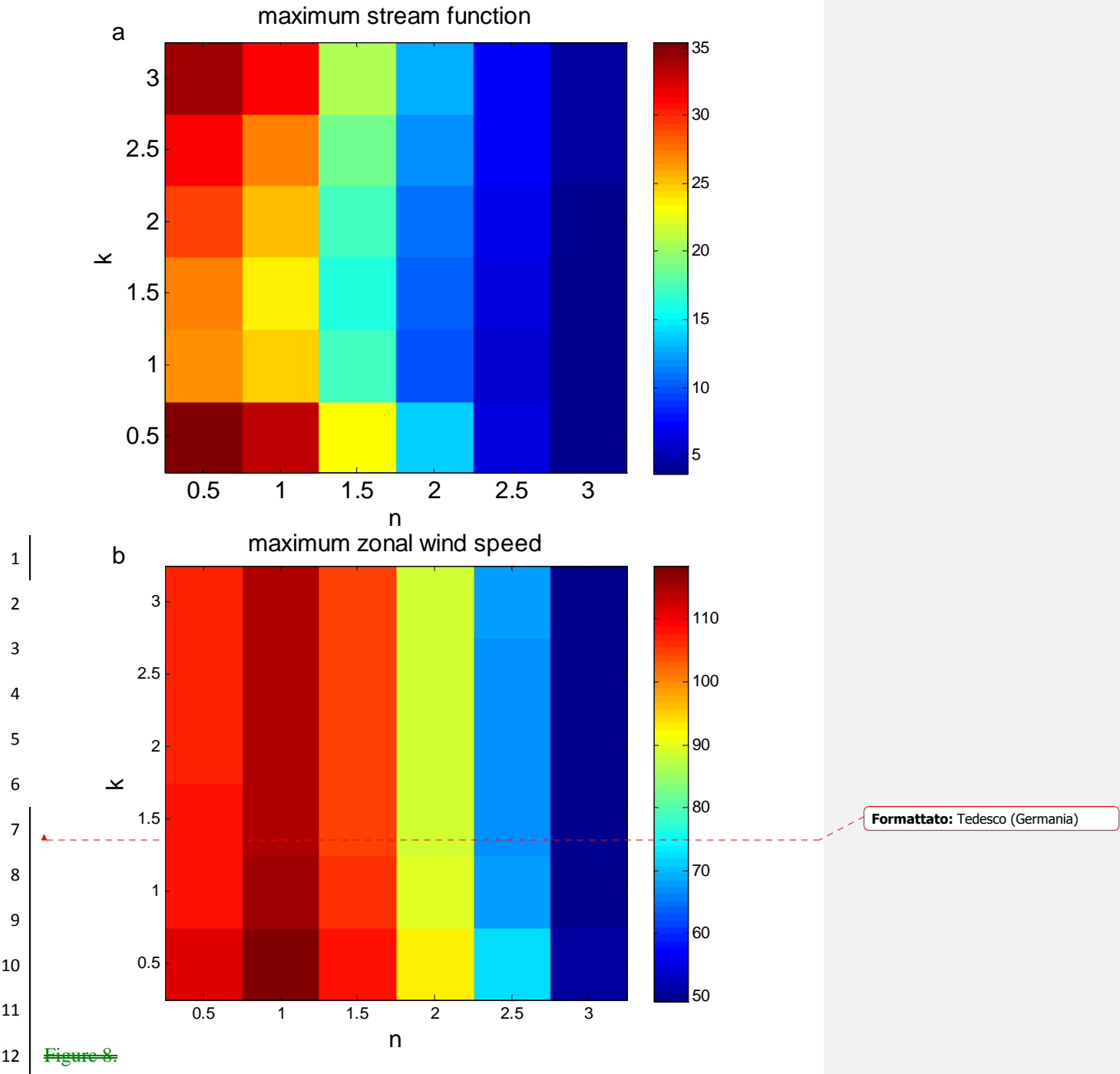
47

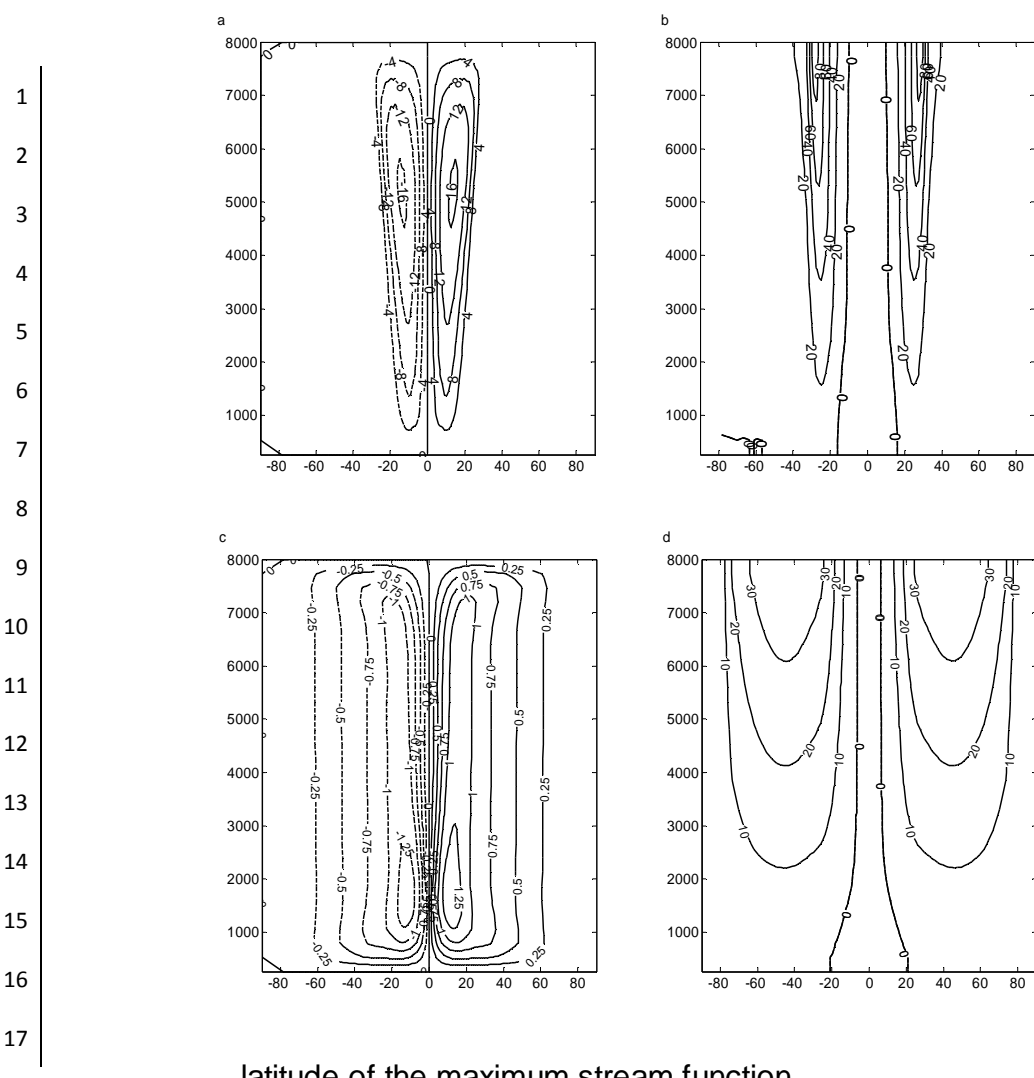
Figur

8.

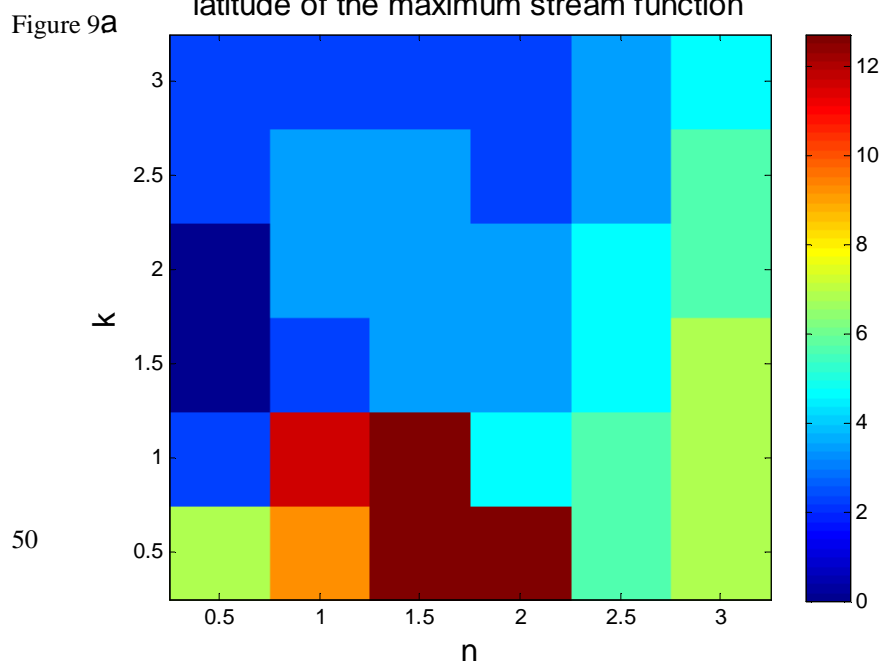
Formattato: Tedesco (Germania)







latitude of the maximum stream function



1

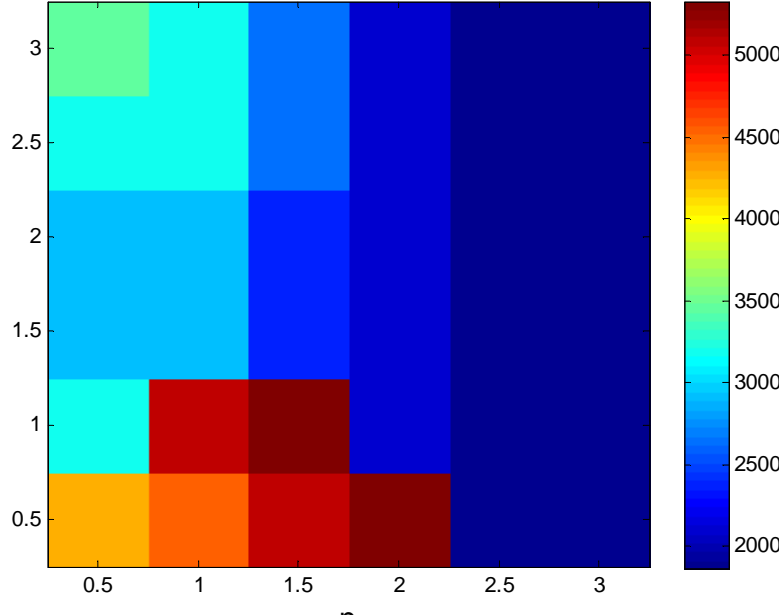
2

3

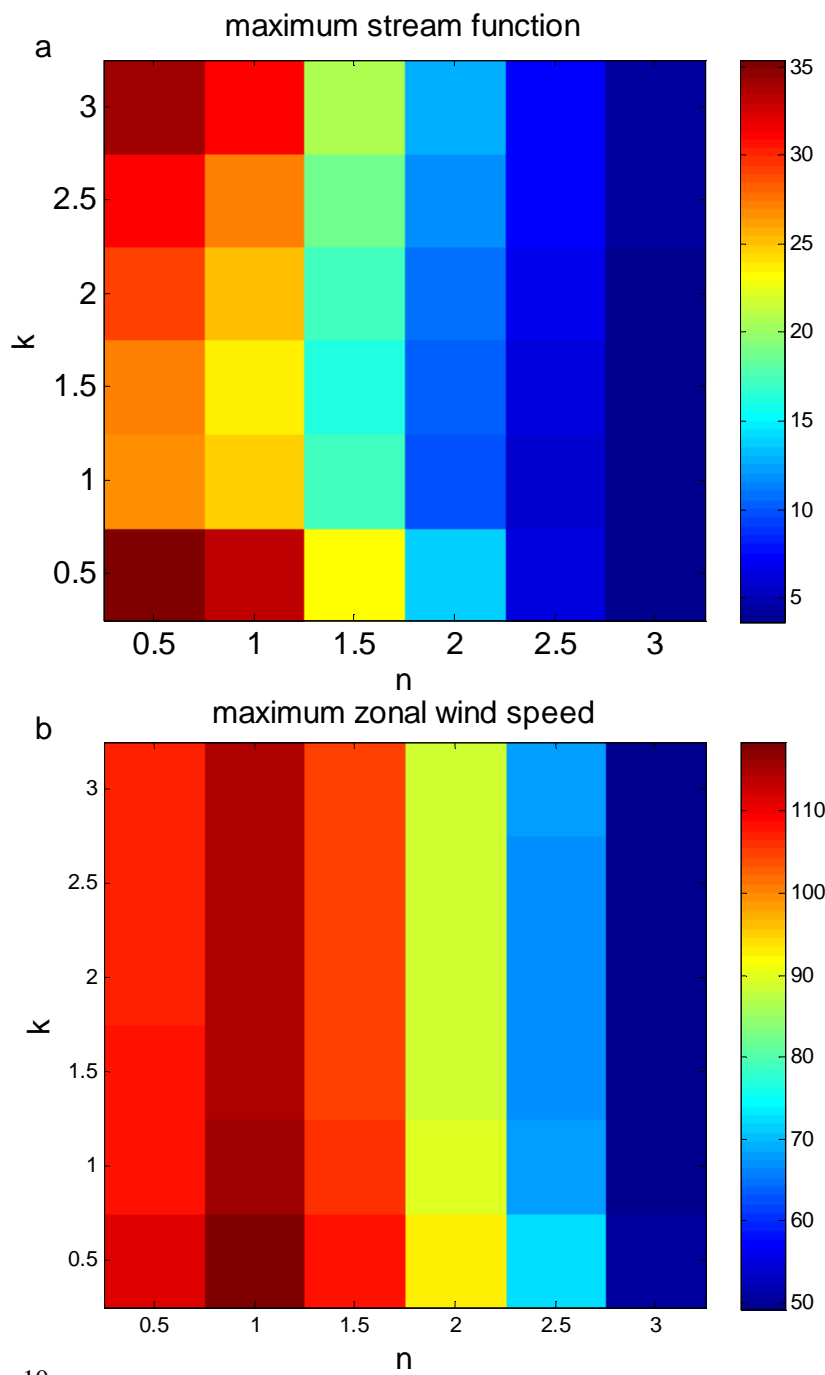
4

b

height of the maximum stream function

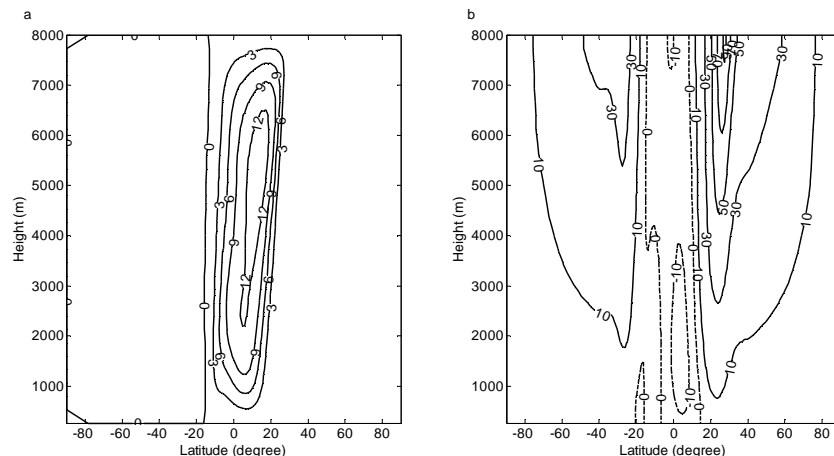


5

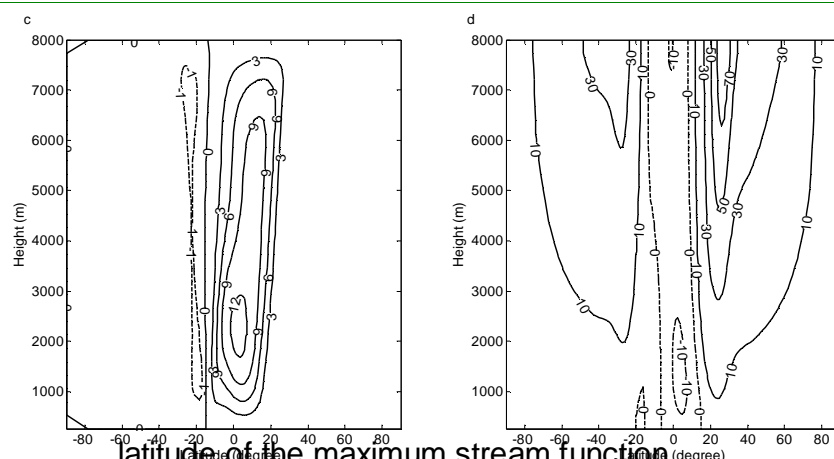


12 Figure 10.

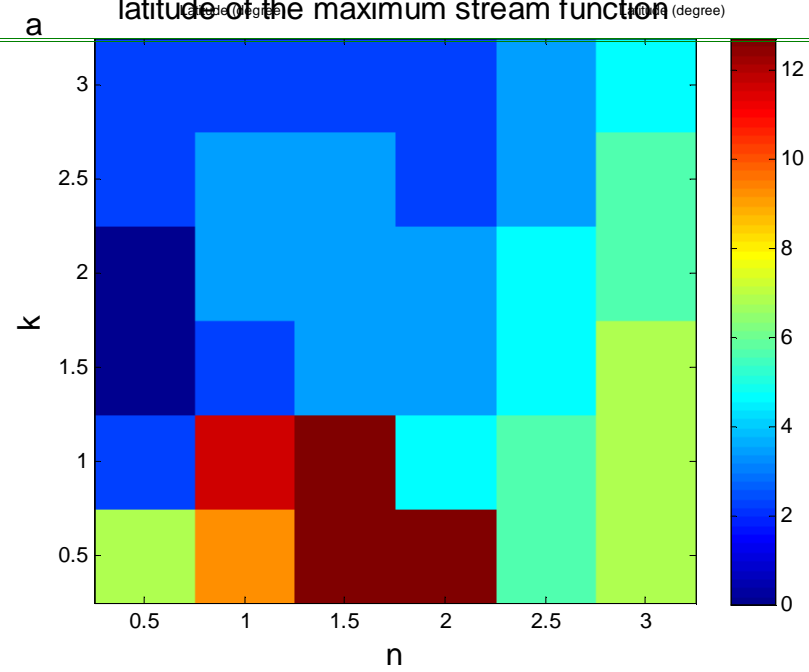
1



2



3



53

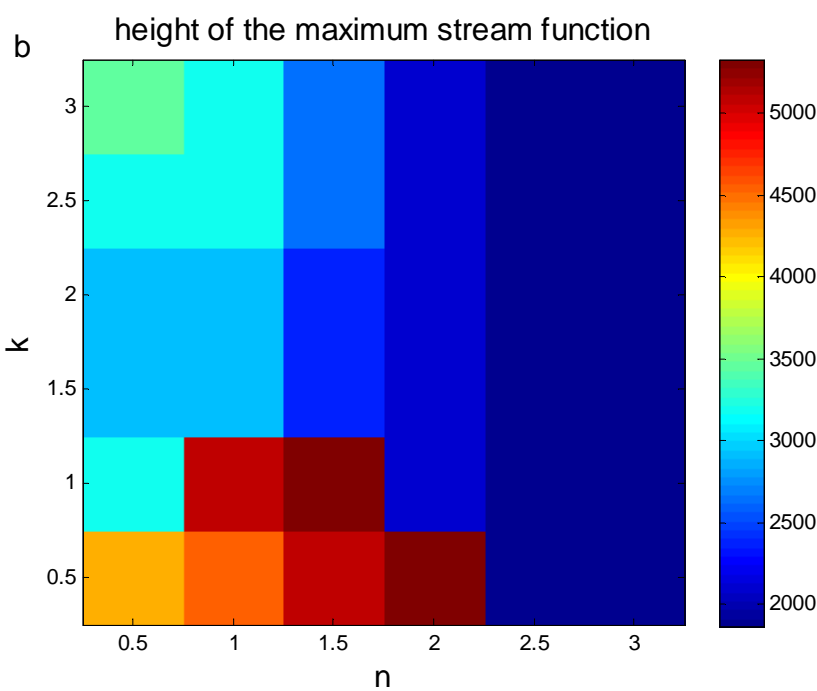
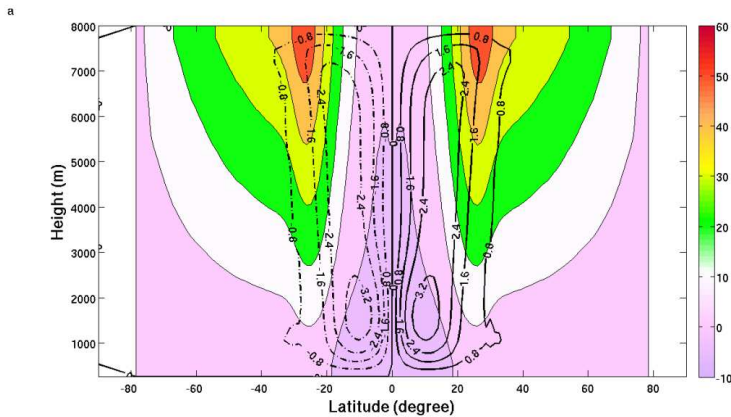
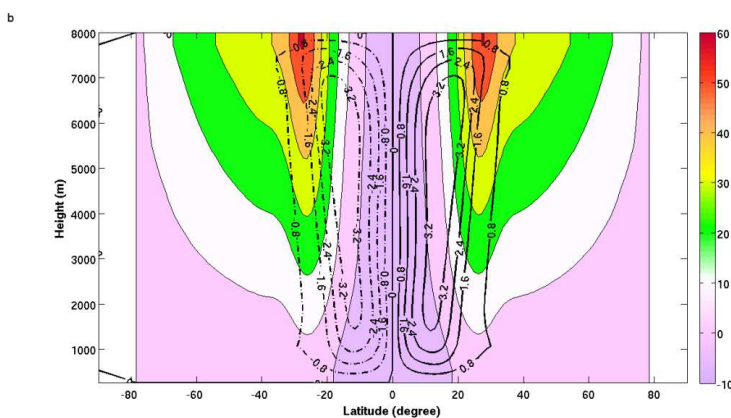


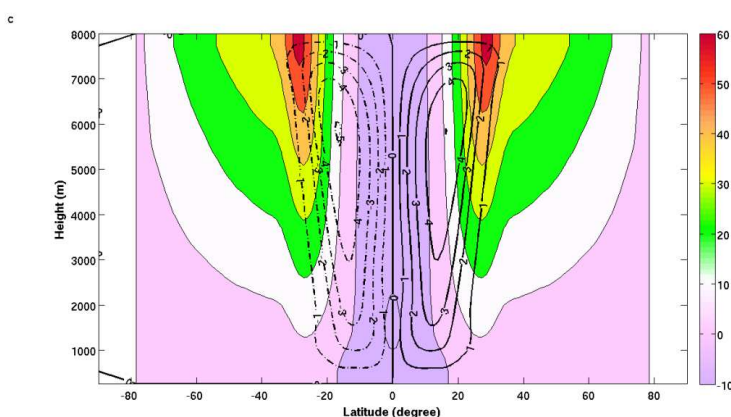
Figure 11.



1

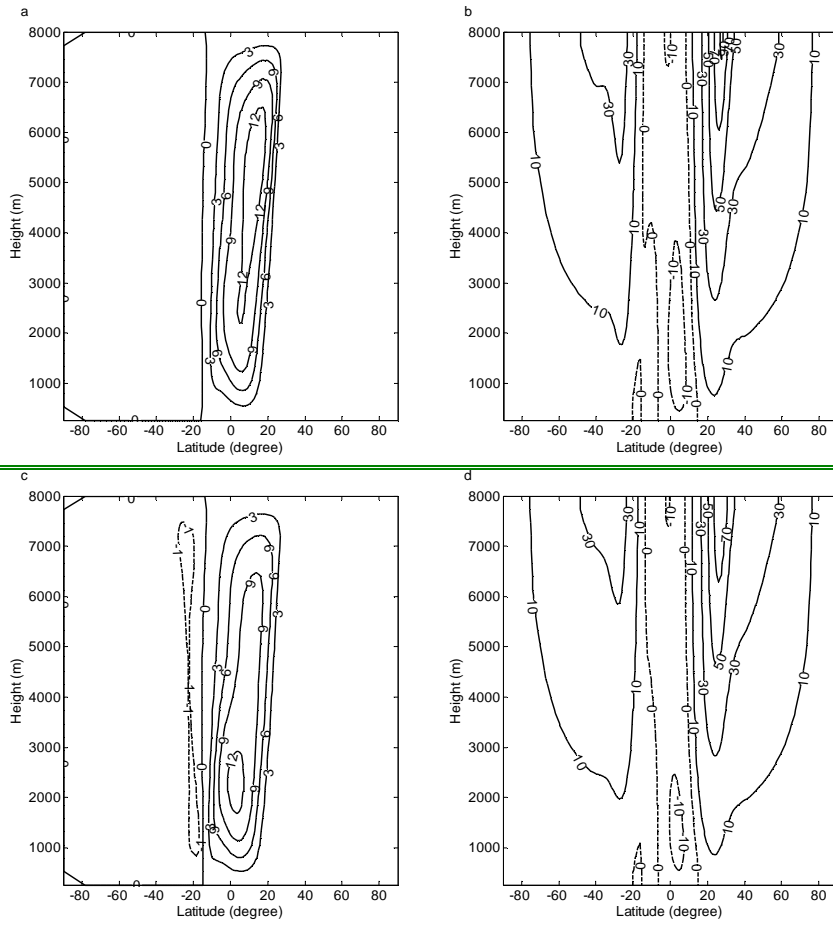


2



3

4



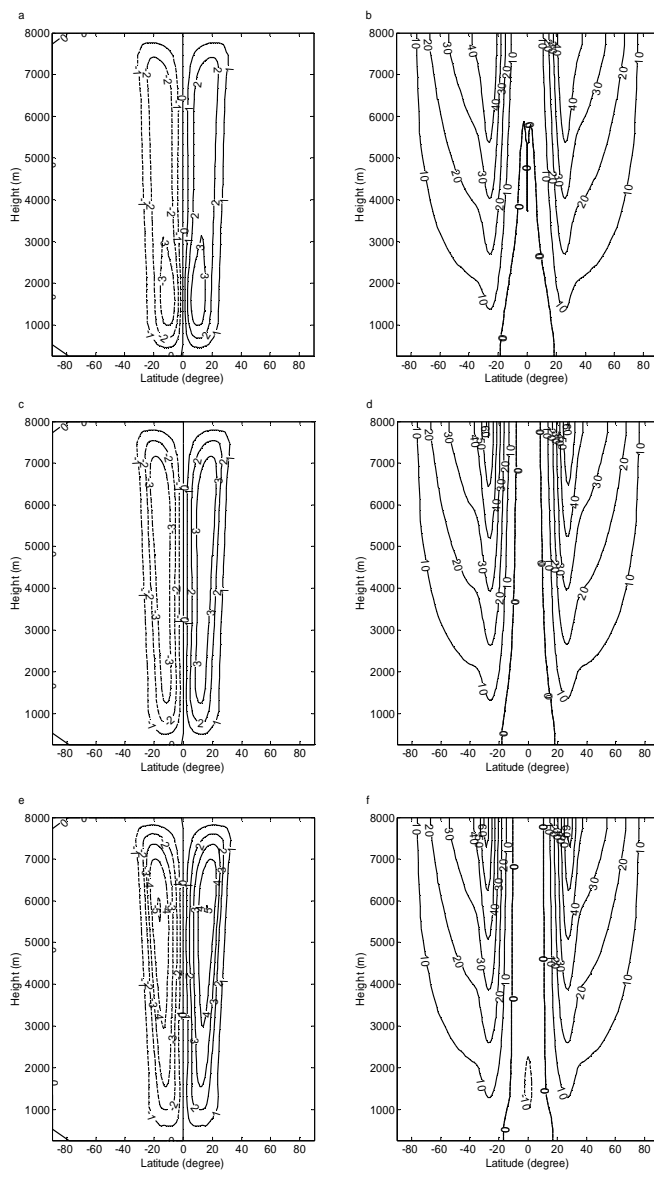


Figure 13.

Formattato: Default Style